

Nonlinear chaotic lattice field theory

S V Williams, M N Gudorf, X Wang, H Liang, and P Cvitanović

School of Physics, Georgia Institute of Technology, Atlanta, GA 30332-0430, USA

E-mail: predrag.cvitanovic@physics.gatech.edu

DRAFT 0.5 February 20, 2025

Abstract. Motivated by [...]

PACS numbers: 02.20.-a, 05.45.-a, 05.45.Jn, 47.27.ed

Keywords: chaotic field theory, many-particle systems, coupled map lattices, periodic orbits, symbolic dynamics, cat maps

Submitted to: *J. Phys. A: Math. Theor.*

1. Introduction

“Amazing! I did not understand a single word!”

And indeed, there is a problem of understanding what is ‘chaos’ [...]

We need to motivate looking at classical ϕ^k theories, I know that there is a big push for ϕ^4 in quantum field theory, so that is likely the best way to go.

2. Deterministic lattice field theory

A scalar field $\phi(x)$ over d Euclidean coordinates can be discretized by replacing the continuous space by a d -dimensional hypercubic integer lattice \mathbb{Z}^d , with lattice spacing  a , and evaluating the field only on the lattice points [38, 40]

$$\phi_z = \phi(x), \quad x = az = \text{lattice point}, \quad z \in \mathbb{Z}^d. \quad (1)$$

A *field configuration* (here in one spatiotemporal dimension)

$$\Phi = \cdots \phi_{-3}\phi_{-2}\phi_{-1}\phi_0\phi_1\phi_2\phi_3\phi_4\cdots, \quad (2)$$

takes any set of values in system’s ∞ -dimensional *state space* $\phi_z \in \mathbb{R}$. A *periodic field configuration* satisfies

$$\Phi_{z+R} = \Phi_z \quad (3)$$

for any discrete translation $R \in \mathcal{L}_{\mathbf{a}}$ in the *Bravais lattice*

$$\mathcal{L}_{\mathbf{a}} = \left\{ \sum_{i=1}^d n_i \mathbf{a}_i \mid n_i \in \mathbb{Z} \right\} = \{ \mathbf{n} \mathbf{A} \mid \mathbf{n} \in \mathbb{Z}^d \} \quad (4)$$

where the matrix \mathbf{A} whose columns are d independent integer lattice vectors \mathbf{a}_j

$$\mathbf{A} = [\mathbf{a}_1, \dots, \mathbf{a}_d] \in \mathbb{R}^{d \times d} \quad (5)$$

defines a *Bravais cell* basis.

The volume of (i.e., the number of lattice sites within) $\mathcal{L}_{\mathbf{a}}$ is defined by the volume of the parallelepiped spanned by the Bravais cell basis

$$N_{\mathbf{a}} \equiv |\det \mathbf{A}|. \quad (6)$$

For example, the periodic orbit for the 1D ϕ^3 , $\overline{10\bar{1}}$, reoccurs for the discrete translation $R = 3$ and this is the only (one dimensional) vector in $\mathcal{L}_{\mathbf{a}}$ so we get the obvious answer that $N_{\mathbf{a}} = 3$ i.e. there are three points in the Bravais cell of this orbit.

The action in (83) is given as Bravais cell sum over the Lagrangian density

$$S_{\mathbf{a}}[\Phi] = \sum_z^{\mathbf{a}} \left\{ \frac{1}{2} \sum_{\mu=1}^d (\partial_{\mu} \phi)_z^2 + V(\phi_z) \right\}, \quad (7)$$

The variational extremum condition (43)

$$F[\Phi_c]_z = \frac{\delta S[\Phi_c]}{\delta \phi_z} = 0, \quad (8)$$

yields the Euler–Lagrange equations of ϕ^k theory (125) on a d -dimensional hypercubic lattice, with *periodic state* Φ_c a global deterministic (or ‘classical’) solution satisfying this local extremal condition on every lattice site z .

Here, and in papers I and II [13, 32] we investigate spatiotemporally chaotic lattice field theories using as illustrative examples the d -dimensional hypercubic lattice (36) discretized Klein-Gordon free-field theory, spatiotemporal cat, spatiotemporal ϕ^3 theory, and spatiotemporal ϕ^4 theory, defined respectively by Euler–Lagrange equations (43)

$$-\square \phi_z + \mu^2 \phi_z = 0, \quad \phi_z \in \mathbb{R}, \quad (9)$$

$$-\square \phi_z + \mu^2 \phi_z - m_z = 0, \quad \phi_z \in [0, 1) \quad (10)$$

$$-\square \phi_z + \mu^2 (1/4 - \phi_z^2) = 0, \quad (11)$$

$$-\square \phi_z + \mu^2 (\phi_z - \phi_z^3) = 0. \quad (12)$$

For free-field theory the sole parameter μ^2 is known as the Klein-Gordon (or Yukawa) mass. The anti-integrable form [2, 3, 48] of the spatiotemporal ϕ^3 (11) and spatiotemporal ϕ^4 (12) Euler–Lagrange equations, and a rescaling away of other ‘coupling’ parameters, is explained below, in sections 14 and 16.

Each periodic state is a distinct deterministic solution Φ_c to the discretized Euler–Lagrange equations (43), so its probability density is a $N_{\mathcal{L}}$ -dimensional Dirac delta

function (that's what we mean by the system being *deterministic*), a delta function per site ensuring that Euler–Lagrange equation (43) is satisfied everywhere, with probability

$$P_c = \frac{1}{Z} \int_{\mathcal{M}_c} d\Phi \delta(F[\Phi]), \quad \Phi_c \in \mathcal{M}_c, \quad (13)$$

where \mathcal{M}_c is an open neighborhood, sufficiently small that it contains only the single periodic state Φ_c .

In [32] we verify that this definition agrees with the forward-in-time Perron-Frobenius probability density evolution [12]. However, we find field-theoretical formulation vastly preferable to the forward-in-time formulation, especially when it comes to higher spatiotemporal dimensions [13].

n -point correlation functions or ‘Green functions’ [44]

$$\langle \phi_i \phi_j \cdots \phi_\ell \rangle = \frac{1}{Z[0]} \int D\phi e^{-S[\phi]} \phi_i \phi_j \cdots \phi_\ell. \quad (14)$$

The deterministic field theory partition sum has support only on lattice field values that are solutions to the Euler–Lagrange equations (43), and the partition function (83) is now a sum over configuration state space (37) *points*, what in theory of dynamical systems is called the ‘deterministic trace formula’ [11],

$$Z[0] = \sum_c P_c = \sum_p \sum_{r=1}^{\infty} P_{p^r}, \quad P_c = \frac{1}{|\text{Det } \mathcal{J}_c|}, \quad (15)$$

and we refer to the $[N_{\mathcal{L}} \times N_{\mathcal{L}}]$ matrix of second derivatives

$$(\mathcal{J}_c)_{z'z} = \frac{\delta F_{z'}[\Phi_c]}{\delta \phi_z} = S[\Phi_c]_{z'z} \quad (16)$$

as the *orbit Jacobian matrix*, and to its determinant $\text{Det } \mathcal{J}_c$ as the *Hill determinant*. Support being on state space *points* means that we do not need to worry about potentials being even or odd (thus unbounded), or the system being energy conserving or dissipative, as long as its nonwandering periodic states Φ_c set is bounded in state space. In what follows, we shall deal only with deterministic field theory and mostly omit the subscript ‘ c ’ in Φ_c .

3. Orbit stability

Solutions of a nonlinear field theory are in general not translation invariant, so the orbit Jacobian matrix (47) (or the ‘discrete Schrödinger operator’ [5, 47])

$$\mathcal{J}_c = \begin{pmatrix} s_0 & -1 & 0 & 0 & \cdots & 0 & -1 \\ -1 & s_1 & -1 & 0 & \cdots & 0 & 0 \\ 0 & -1 & s_2 & -1 & \cdots & 0 & 0 \\ \vdots & \vdots & \vdots & \vdots & \ddots & \vdots & \vdots \\ 0 & 0 & 0 & 0 & \cdots & s_{n-2} & -1 \\ -1 & 0 & 0 & 0 & \cdots & -1 & s_{n-1} \end{pmatrix} \quad (17)$$

is not a circulant matrix: each periodic state Φ_c has its own orbit Jacobian matrix $\mathcal{J}_c = \mathcal{J}[\Phi_c]$, with the ‘stretching factor’ $s_t = V''(\phi_t) + 2$ at the lattice site t a function of the site field ϕ_t .

The orbit Jacobian matrix of a period- (mn) periodic state Φ , which is a m -th *repeat* of a period- n prime periodic state Φ_p , has a tri-diagonal block circulant matrix form that follows by inspection from (98):

$$\mathcal{J}_{p^r} = \begin{pmatrix} \mathbf{s}_p & -\mathbf{r} & & & -\mathbf{r}^\top \\ -\mathbf{r}^\top & \mathbf{s}_p & -\mathbf{r} & & \\ & \ddots & \ddots & \ddots & \\ & & -\mathbf{r}^\top & \mathbf{s}_p & -\mathbf{r} \\ -\mathbf{r} & & & -\mathbf{r}^\top & \mathbf{s}_p \end{pmatrix}, \quad (18)$$

where block matrix \mathbf{s}_p is a $[n \times n]$ symmetric Toeplitz matrix

$$\mathbf{s}_p = \begin{pmatrix} s_0 & -1 & & & 0 \\ -1 & s_1 & -1 & & \\ & \ddots & \ddots & \ddots & \\ & & -1 & s_{n-2} & -1 \\ 0 & & & -1 & s_{n-1} \end{pmatrix}, \quad \mathbf{r} = \begin{pmatrix} 0 & \cdots & 0 \\ & \ddots & \vdots \\ 1 & & 0 \end{pmatrix}, \quad (19)$$

and \mathbf{r} and its transpose enforce the periodic bc’s. This period- (mn) periodic state Φ orbit Jacobian matrix is as translation-invariant as the temporal cat, but now under Bravais lattice translations by multiples of n . One can visualize this periodic state as a tiling of the integer lattice \mathbb{Z} by a generic periodic state field decorating a tile of length n . The orbit Jacobian matrix \mathcal{J} is now a block circulant matrix which can be brought into a block diagonal form by a unitary transformation, with a repeating $[n \times n]$ block along the diagonal.

4. Observables

2022-01-19, 2023-02-11 Predrag Because of the dependence of the orbit Jacobian matrix (99) on the primitive cell \mathbf{A} repeat number r , we have to distinguish the partition function $Z_{\mathbf{A}}$ defined over the finite lattice volume $N_{\mathcal{L}} = N_{\mathbf{A}}$ primitive cell from the (infinite) lattice partition function $Z_{\mathcal{L}}$, which is the sum over all distinct primitive cells.

A field configuration Φ over a primitive cell \mathbf{A} of lattice \mathcal{L} occurs with probability density

$$P_{\mathbf{A}}[\Phi] = \frac{1}{Z} e^{-S_{\mathbf{A}}[\Phi]}, \quad Z = Z_{\mathcal{L}}[0]. \quad (20)$$

Here $Z_{\mathcal{L}}$ is a normalization factor, given by the *partition sum*, the sum (in continuum, the integral) over probabilities of all configurations,

$$Z_{\mathcal{L}}[J] = e^{N_{\mathcal{L}}W_{\mathcal{L}}} = \int_{\mathcal{L}} d\Phi P[\Phi] e^{\Phi \cdot J}, \quad d\Phi = \prod_z^{\mathcal{L}} d\phi_z, \quad (21)$$

where $\mathbf{J} = \{j_z\}$ is an external source j_z that one can vary site by site, and $S[\Phi]$ is the action that defines the theory (discussed in more detail in section ??). The dimension of the partition function integral equals the number of lattice sites $N_{\mathcal{L}}$, i.e., the lattice volume (41).

Birkhoff sum [30] over primitive cell c

$$A_c = \sum_{z \in c} a_z. \quad (22)$$

Birkhoff average over primitive cell c

$$\langle a \rangle_c = \frac{A_c}{N_c}. \quad (23)$$

The free energy (the large-deviation potential?)

$$\begin{aligned} Z_{\mathbf{A}}[0] &= \sum_c e^{N_{\mathcal{L}} W_c[0]} \\ e^{N_{\mathcal{L}} W_c[0]} &= \int_{\mathcal{M}_c} d\Phi \delta(F[\Phi]) = \frac{1}{|\text{Det } \mathcal{J}_c|} \end{aligned} \quad (24)$$

was originally snuck into (15) (see (??), (??), (??)) See also partition function (??), (??), (??); partition sum (??); Ising (??); Gaussian (??).

5. Nonlinear lattice field theory

As we are writing this as a primer to our methods geared towards nonlinear lattice field theories, we choose to consider the most structurally simple of nonlinearities: Euclidean ϕ^k theory. First, we examine a continuum scalar, one-component field, d -dimensional Euclidean ϕ^k theory defined by action [28, 42, 53]

$$S[\Phi] = \int d^d x \left\{ \frac{1}{2} [\partial_\mu \phi(x)]^2 + \frac{\mu^2}{2} \phi^2(x) - \frac{g}{k!} \phi^k(x) \right\}, \quad (25)$$

with the Klein-Gordon mass $\mu \geq 0$, and the strength of the self-coupling $g \geq 0$. When working with nonlinear systems, we are really only interested in unstable orbits. As this is the case, we have chosen our action to have the ϕ^k potential inverted when compared to more classical treatments. 

When working on a discretized ϕ^k theory, the action is defined as the lattice sum over the Euclidean Lagrangian density and (123) becomes [39]

$$S[\Phi] = \sum_z \left\{ \frac{1}{2} \sum_{\mu=1}^d (\partial_\mu \phi)_z^2 + \frac{\mu^2}{2} \phi_z^2 - \frac{g}{k!} \phi_z^k \right\}, \quad (26)$$

where we have set lattice constant $a = 1$ throughout. In the spirit of anti-integrability [3], we split the action into ‘kinetic’ and local ‘potential’ parts $S[\Phi] = -\frac{1}{2} \Phi^\top \square \Phi + V[\Phi]$, where the nonlinear self-interaction is contained in

$$V[\Phi] = \sum_z V(\phi_z), \quad V(\phi) = \frac{1}{2} \mu^2 \phi^2 - \frac{g}{k!} \phi^k, \quad k \geq 3 \quad (27)$$

with $V(\phi_z)$ a nonlinear potential, intrinsic to the lattice site z . The part bilinear in fields is the free field theory action

$$S_0[\Phi] = \frac{1}{2} \Phi^\top (-\square + \mu^2 \mathbf{1}) \Phi, \quad (28)$$

Here the lattice Laplacian

$$\square \phi_z = \sum_{\|z'-z\|=1} (\phi_{z'} - \phi_z) = -2d \phi_z + \sum_{\|z'-z\|=1} \phi_{z'} \quad \text{for all } z, z' \in \mathcal{L} \quad (29)$$

is the average of the lattice field variation $\phi_{z'} - \phi_z$ over the sites nearest to the site z . For a hypercubic lattice in one and two dimensions this discretized Laplacian is given by

$$\square \phi_t = \phi_{t+1} - 2\phi_t + \phi_{t-1} \quad (30)$$

$$\square \phi_{jt} = \phi_{j,t+1} + \phi_{j+1,t} - 4\phi_{jt} + \phi_{j,t-1} + \phi_{j-1,t}. \quad (31)$$

As we have now defined an action, we can write down the lattice Euler Lagrange equation which we can solve with periodic boundary conditions in order to determine the periodic orbits central to our theories of nonlinear dynamics.

First, we note that $\square \equiv -\partial^T \partial$ because \square is the lattice Laplacian which, in finite difference notation, is given by $\square = \frac{1}{a^2} (\sigma^{-1} - 2I - \sigma)$ and $\partial^T \partial = \frac{1}{a^2} (\sigma^{-1} - I) (\sigma - I) = \frac{1}{a^2} (2I - \sigma - \sigma^{-1})$. Where σ is a matrix which rotates the lattice state forward by one lattice point. Now, if we take.

$$(\partial_\mu \phi)^T \partial_\mu \phi = \phi \partial_\mu^T \partial_\mu \phi = -\phi \square \phi \quad (32)$$

Using (32) we can write our action (124) as

$$S[\phi] = \sum_\mu \frac{1}{2} (\partial_\mu \phi)^2 + V(\phi) = \sum_\mu -\frac{1}{2} \phi \square \phi + V(\phi) \quad (33)$$

This should encompass all our Hamiltonian field theories (those that are non-dissipative can be treated through an action formulation). Now, the functional derivative commutes with the partial derivatives present in \square , and \square is self-adjoint, so it works the same acting from the right as it does acting from the left. Therefore, we can write

$$\frac{\delta S[\phi]}{\delta \phi} = \sum_\mu -\frac{1}{2} \phi \square - \frac{1}{2} \square \phi + V'(\phi) = 0 \quad (34)$$

Summing over independent directions to get zero implies that each member of the sum is zero, so we get

$$-\square \phi + V'(\phi) = 0 \quad (35)$$

as our lattice Euler–Lagrange equations.

We will be closely investigating two ϕ^k theories: the aforementioned ϕ^4 , and ϕ^3 . ϕ^4 has wide application in quantum field theory [needs citations](#) and thus understanding its behavior from a nonlinear dynamics perspective would be extremely useful. ϕ^3 on the other hand, is less useful for qft due to the non-normalizability of its potential, but its close connection to the well-studied temporal Hénon ([Appendix A](#)) allows us

to explore many properties analytically, and even draw global conclusions about our field theory formulation in general. This paper will exclusively concern itself with one-dimensional theories, this follows along with our effort to build up understanding of chaotic spatiotemporal field theories in chunks [cite LC21 and CL18](#). In the following sections we develop both ϕ^3 and ϕ^4 from (124), some general properties of each theory are developed followed by a discussion on "shadow states" and the symmetries of each system. With all this information, we are able to use Newton's method to extremely accurately and quickly determine cycles of up to length ?? for each theory.

6. Deterministic lattice field theory

A scalar field $\phi(x)$ over d Euclidean coordinates can be discretized by replacing the continuous space by a d -dimensional hypercubic integer lattice \mathbb{Z}^d , with lattice spacing a , and evaluating the field only on the lattice points [\[38, 40\]](#) 

$$\phi_z = \phi(x), \quad x = az = \text{lattice point}, \quad z \in \mathbb{Z}^d. \quad (36)$$

A *field configuration* (here in one spatiotemporal dimension)

$$\Phi = \cdots \phi_{-3} \phi_{-2} \phi_{-1} \phi_0 \phi_1 \phi_2 \phi_3 \phi_4 \cdots, \quad (37)$$

takes any set of values in system's ∞ -dimensional *state space* $\phi_z \in \mathbb{R}$. A periodic field configuration satisfies

$$\Phi_{z+R} = \Phi_z \quad (38)$$

for any discrete translation $R \in \mathcal{L}_{\mathbf{a}}$ in the *Bravais lattice*

$$\mathcal{L}_{\mathbf{a}} = \left\{ \sum_{i=1}^d n_i \mathbf{a}_i \mid n_i \in \mathbb{Z} \right\} = \{ \mathbf{n} \mathbf{A} \mid \mathbf{n} \in \mathbb{Z}^d \} \quad (39)$$

(2023-02-11 Predrag Wrong: if \mathbf{n} is a row vector, \mathbf{a}_j should also be row vectors.)

where the matrix \mathbf{A} whose columns are d independent integer lattice vectors \mathbf{a}_j

$$\mathbf{A} = [\mathbf{a}_1, \cdots, \mathbf{a}_d] \in \mathbb{R}^{d \times d} \quad (40)$$

defines a *primitive cell* basis.

The determinant of lattice $\mathcal{L}_{\mathbf{a}}$ is the volume of (i.e., the number of lattice sites within) the parallelepiped spanned by the primitive cell basis

$$N_{\mathbf{a}} = |\det \mathbf{A}|. \quad (41)$$

The action in (??) is given as primitive cell sum over the Lagrangian density

$$S_{\mathbf{a}}[\Phi] = \sum_z^{\mathbf{a}} \left\{ \frac{1}{2} \sum_{\mu=1}^d (\partial_{\mu} \phi)_z^2 + V(\phi_z) \right\}, \quad (42)$$

The variational extremum condition [\(43\)](#)

$$F[\Phi_c]_z = \frac{\delta S[\Phi_c]}{\delta \phi_z} = 0, \quad (43)$$

yields the Euler–Lagrange equations of ϕ^k theory (125) on a d -dimensional hypercubic lattice, with *periodic state* Φ_c a global deterministic (or ‘classical’) solution satisfying this local extremal condition on every lattice site z .

Each periodic state is a distinct deterministic solution Φ_c to the discretized Euler–Lagrange equations (43), so its probability density is a $N_{\mathcal{L}}$ -dimensional Dirac delta function (that’s what we mean by the system being *deterministic*), a delta function per site ensuring that Euler–Lagrange equation (43) is satisfied everywhere, with probability

$$P_c = \frac{1}{Z} \int_{\mathcal{M}_c} d\Phi \delta(F[\Phi]), \quad \Phi_c \in \mathcal{M}_c, \quad (44)$$

where \mathcal{M}_c is an open neighborhood, sufficiently small that it contains only the single periodic state Φ_c .

In [32] we verify that this definition agrees with the forward-in-time Perron–Frobenius probability density evolution [12]. However, we find field-theoretical formulation vastly preferable to the forward-in-time formulation, especially when it comes to higher spatiotemporal dimensions [13].

n -point correlation functions or ‘Green functions’ [44]

$$\langle \phi_i \phi_j \cdots \phi_\ell \rangle = \frac{1}{Z[0]} \int D\phi e^{-S[\phi]} \phi_i \phi_j \cdots \phi_\ell. \quad (45)$$

The deterministic field theory partition sum has support only on lattice field values that are solutions to the Euler–Lagrange equations (43), and the partition function (83) is now a sum over configuration state space (37) *points*, what in theory of dynamical systems is called the ‘deterministic trace formula’ [11],

$$Z[0] = \sum_c P_c = \sum_p \sum_{r=1}^{\infty} P_{p^r}, \quad P_c = \frac{1}{|\text{Det } \mathcal{J}_c|}, \quad (46)$$

and we refer to the $[N_{\mathcal{L}} \times N_{\mathcal{L}}]$ matrix of second derivatives

$$(\mathcal{J}_c)_{z'z} = \frac{\delta F_{z'}[\Phi_c]}{\delta \phi_z} = S[\Phi_c]_{z'z} \quad (47)$$

as the *orbit Jacobian matrix*, and to its determinant $\text{Det } \mathcal{J}_c$ as the *Hill determinant*. Support being on state space *points* means that we do not need to worry about potentials being even or odd (thus unbounded), or the system being energy conserving or dissipative, as long as its nonwandering periodic states Φ_c set is bounded in state space. In what follows, we shall deal only with deterministic field theory and mostly omit the subscript ‘ c ’ in Φ_c .

7. A partition function in terms of prime periodic states

See also section ?? *Repeats of a prime primitive cell*.

A single *prime* periodic state Φ_p over primitive cell \mathbb{A} has the same Hill determinant and Birkhoff sum $A_{\mathbb{A}}[\Phi_p]$ for the $N_{\mathbb{A}}$ periodic states in its group orbit, so its contribution to the partition function (15) is

$$e^{N_p W_{\mathbb{A}}[\beta]_p} = \frac{N_p}{|\text{Det}_{\mathbb{A}} \mathcal{J}_p|} e^{\beta N_p a_p}, \quad N_p = N_{\mathbb{A}} = L_{\mathbb{A}} T_{\mathbb{A}}, \quad (48)$$

For the prime periodic state Φ_p over a *repeated* primitive cell tile $\mathbb{A}\mathbb{R}$ (??), the contribution to the partition function is

$$e^{N_{\mathbb{A}\mathbb{R}}W_{\mathbb{A}\mathbb{R}}[\beta]_p} = \frac{N_p}{|\text{Det}_{\mathbb{A}\mathbb{R}}\mathcal{J}_p|} e^{\beta N_{\mathbb{A}\mathbb{R}}a_p}, \quad N_{\mathbb{A}\mathbb{R}} = r_1 r_2 N_p. \quad (49)$$

The nuisance here is that the Hill determinant $\text{Det}_{\mathbb{A}\mathbb{R}}\mathcal{J}_p$ has no simple multiplicative relation to $\text{Det}_{\mathbb{A}}\mathcal{J}_p$; has to be computed for each repeat separately, though in the infinite lattice limit they all might get replaced by a band in the first Brillouin zone.

Summing over all prime orbit p repeats (all $\mathbb{A}\mathbb{R}$ primitive cells), we have the p contribution to the partition sum

$$Z[\beta]_p = e^{N_p W[\beta]_p} = \sum_{r_1=1}^{\infty} \sum_{r_2=1}^{\infty} \frac{N_p}{|\text{Det}_{\mathbb{A}\mathbb{R}}\mathcal{J}_p|} e^{\beta r_1 r_2 N_p a_p}, \quad (50)$$

and to the expectation value of observable $a_z = a(\phi_z)$

$$\langle a \rangle_p = \frac{1}{N_p} \left. \frac{\partial}{\partial \beta} W[\beta]_p \right|_{\beta=0} = a_p w'_p, \quad w'_p = \frac{1}{Z_p} \sum_{r_1=1}^{\infty} \sum_{r_2=1}^{\infty} \frac{r_1 r_2}{|\text{Det}_{\mathbb{A}\mathbb{R}}\mathcal{J}_p|}. \quad (51)$$

Finally, summing over all prime orbits we have the mother of spatiotemporal partition functions and expectation values

$$Z[\beta] = e^{W[\beta]} = \sum_p e^{N_p W[\beta]_p}, \quad \langle a \rangle = \sum_p a_p w_p. \quad (52)$$

Prime orbits p are themselves searched for and ordered by the hierarchy of primitive cells

$$\sum_p \cdots = \sum_{r_1=1}^{\infty} \sum_{r_2=1}^{\infty} \sum_{r_3=0}^{r_1-1} \cdots, \quad (53)$$

Now, all this is what ChaosBook calls a ‘trace formula’, everything contributes to orbit weights w_p with positive signs, there are *no shadowing cancellations*. For that one needs a cumulant expansion of the Helmholtz ‘free energy’ $W[\beta] = \ln Z[\beta]$.

And all stability calculations have to be done in the first Brillouin zone.

I’ll be grateful if you do it, but if not, I’ll try.

7.1. Retiling the tiles, ver. 2023-02-28

2023-02-12 Predrag This section or similar goes into Han’s thesis, we have replaced it in CL18 by sect. *Tile multiples*.

A Bravais lattice $\mathcal{L}_{\mathbb{A}}$ is a sublattice of a Bravais lattice $\mathcal{L}_{\mathbb{B}}$ if its primitive vectors are integer multiples of the $\mathcal{L}_{\mathbb{B}}$ primitive vectors [16],

$$\mathbb{A} = \mathbb{B}\mathbb{M}, \quad |\det \mathbb{B}| > 1, \quad |\det \mathbb{M}| > 1. \quad (54)$$

We now reformulate this as a condition on which primitive cells \mathbb{B} can tile a primitive cell \mathbb{A} , see figure ??.

Bravais lattices $\mathcal{L}_{\mathbb{A}} = [L_a \times T_a]_{S_a}$, $\mathcal{L}_{\mathbb{B}} = [L_b \times T_b]_{S_b}$, and the integer multipliers of lattice $\mathcal{L}_{\mathbb{B}}$ are given by Hermite normal form primitive vectors (60)

$$\mathbb{A} = \begin{bmatrix} L_a & S_a \\ 0 & T_a \end{bmatrix}, \quad \mathbb{B} = \begin{bmatrix} L_b & S_b \\ 0 & T_b \end{bmatrix}, \quad \mathbb{M} = \begin{bmatrix} r_1 & m_{12} \\ 0 & r_2 \end{bmatrix}. \quad (55)$$

It follows from (54) that the primitive cell \mathbb{B} tiles the primitive cell \mathbb{A} if and only if

$$\mathbb{M} = \mathbb{B}^{-1}\mathbb{A} = \begin{bmatrix} L_a/L_b & (S_a T_b - S_b T_a)/L_b T_b \\ 0 & T_a/T_b \end{bmatrix} \quad (56)$$

is a matrix with integer elements, i.e., only if L_a is a multiple of L_b , T_a is a multiple of T_b , and the area spanned by the two ‘tilted’ primitive vectors (see figure ?? (a))

$$S_a T_b - T_a S_b = \det[\mathbf{a}_2, \mathbf{b}_2] \quad (57)$$

is an integer multiple of the $\mathcal{L}_{\mathbb{B}}$ primitive cell area $L_b T_b$.

As a simple but perhaps surprising example, consider $\mathcal{L} = [2 \times 2]_0$, $\mathcal{L}_{\mathbf{p}} = [2 \times 1]_1$. The Bravais lattice $[2 \times 2]_0$ is a sublattice of $[2 \times 1]_1$, since

$$\begin{bmatrix} L/L_p & S/L_p - S_p T/L_p T_p \\ 0 & T/T_p \end{bmatrix} = \begin{bmatrix} 1 & -1 \\ 0 & 2 \end{bmatrix} \quad (58)$$

is an integer matrix (see also section ??).

Figure ?? is another example of such tiling of a Bravais sublattice primitive cell by a finer Bravais lattice primitive cell. Bravais lattice $[3 \times 2]_1$ (red dots) is a subset of Bravais lattice $[3 \times 1]_2$ (blue and red dots). Figure ?? (b) shows that one can choose primitive cells for these two lattices such that the primitive cell of $[3 \times 2]_1$ is tiled by the primitive cell of $[3 \times 1]_2$, using a translation of $[3 \times 1]_2$.

\mathbb{B} is not necessarily the smallest tile that tiles the primitive cell \mathbb{A} . If $|\det \mathbb{B}|$ is not a prime number, the above procedure can be repeated, tiling the primitive cell \mathbb{B} by repeats of a smaller tile. And the smallest possible tile, the integer lattice \mathbb{Z}^2 unit square tiles any larger tile.

7.2. Retiling the tiles, ver. 2023-01-19

For the temporal cat and spatiotemporal cat, the 1-dimensional fields is defined on the sites of the d -dimensional (hyper-cubic) integer lattice \mathbb{Z}^d . So the periodicities can only be given by lattices with integer components, i.e., a sublattice of \mathbb{Z}^d . To make $\mathcal{L}_{\mathbf{a}}$ a sublattice of \mathbb{Z}^d the basis must only consist of integers,

$$\mathbf{A} = [\mathbf{a}_1, \dots, \mathbf{a}_d] \in \mathbb{Z}^{d \times d}. \quad (59)$$

For a 2-dimensional lattice, the choice of lattice basis $\mathbf{A} \in \mathbb{Z}^{2 \times 2}$ is not unique. The infinity of equivalent bases are related by unimodular transformations [46]: $\mathcal{L}_{\mathbf{a}} = \mathcal{L}_{\mathbf{b}}$ if and only if $\mathbf{A} = \mathbf{B}\mathbf{U}$, where $\mathbf{U} \in \mathbb{Z}^{2 \times 2}$ and $\det \mathbf{U} = \pm 1$. Nevertheless, each 2-dimensional lattice has a unique *Hermite normal form* [10] basis,

$$\mathbf{A} = \begin{bmatrix} L & S \\ 0 & T \end{bmatrix}, \quad (60)$$

where L , T are respectively the spatial, temporal lattice periods, and the ‘tilt’ [41] $0 \leq S < L$ imposes the relative-periodic ‘shift’bc’s). We label the lattice \mathcal{L}_a with \mathbf{A} in Hermite normal form (60) by $[L \times T]_S$. An example of the $[3 \times 2]_1$ lattice is shown in figure ??.

A lattice \mathcal{L}_a is a sublattice of lattice \mathcal{L}_b if and only if the basis of \mathcal{L}_a is in the lattice \mathcal{L}_b , i.e.,

$$\mathbf{A} = \mathbf{B}\mathbf{Q}, \quad \mathbf{Q} \in \mathbb{Z}^{2 \times 2}. \quad (61)$$

If \mathcal{L}_a is a sublattice of \mathcal{L}_b , we can choose the fundamental domain of \mathcal{L}_b that can tile the fundamental domain of \mathcal{L}_a .

If $|\det \mathbf{A}|$ is not a prime number or 1, it can be decomposed into the product of two integer matrices: $\mathbf{A} = \mathbf{B}\mathbf{Q}$, where neither \mathbf{B} nor \mathbf{Q} is unimodular [16]. So if $|\det \mathbf{A}|$ is not a prime number or 1, \mathcal{L}_a is a sublattice of a lattices other than the integer lattice \mathbb{Z}^2 . If $|\det \mathbf{A}|$ is a prime number, \mathcal{L}_a is not a sublattice of other lattices except for the integer lattice \mathbb{Z}^2 and we call \mathcal{L}_a prime lattice. If $|\det \mathbf{A}|$ is 1, \mathcal{L}_a is \mathbb{Z}^2 .

Write the basis of \mathcal{L}_a and \mathcal{L}_b in the Hermite normal form:

$$\mathbf{A} = \begin{bmatrix} \mathbf{a}_1 & \mathbf{a}_2 \end{bmatrix} = \begin{bmatrix} L_a & S_a \\ 0 & T_a \end{bmatrix}, \quad \mathbf{B} = \begin{bmatrix} \mathbf{b}_1 & \mathbf{b}_2 \end{bmatrix} = \begin{bmatrix} L_b & S_b \\ 0 & T_b \end{bmatrix}. \quad (62)$$

By (61), $\mathbf{Q} = \mathbf{B}^{-1}\mathbf{A}$ is an integer matrix if \mathcal{L}_a is a sublattice of \mathcal{L}_b , and this is satisfied only if L_a is a multiple of L_b , T_a is a multiple of T_b , and the two tile ‘tilts’ satisfy that the area spanned by the two ‘tilted’ primitive vectors

$$\det \begin{bmatrix} \mathbf{a}_2 & \mathbf{b}_2 \end{bmatrix} = S_a T_b - T_a S_b \quad (63)$$

is a multiple of the \mathcal{L}_b tile area $L_b T_b$.

A given *Bravais lattice* \mathcal{L} can be defined by any of the infinity of primitive cells, each defined by a different pair of primitive vectors $(\mathbf{a}_1, \mathbf{a}_2)$, but equivalent under unimodular, $\text{SL}(2, \mathbb{Z})$ transformation [31]. Each such family contains a unique primitive cell of the *Hermite normal form* [10], which, for a 2-dimensional square lattice, can be chosen to have the first primitive vector pointing in the spatial direction [34]

$$\mathbf{a}_1 = \begin{pmatrix} L \\ 0 \end{pmatrix}, \quad \mathbf{a}_2 = \begin{pmatrix} S \\ T \end{pmatrix}, \quad (64)$$

where L , T are respectively the spatial, temporal lattice periods, and the ‘tilt’ [41] $0 \leq S < L$ imposes the relative-periodic ‘shift’ bc’s [11] (in the integer lattices literature these are also referred to as ‘helical’ [33] vs. ‘toroidal’ [27]; ‘twisted’ and ‘twisting factor’ [33]; ‘screw’ bc’s). We label primitive cell (64) and the corresponding Bravais lattice \mathcal{L} by $[L \times T]_S$. An example is the $[3 \times 2]_1$ Bravais lattice is shown in reffig f:BravaisLatt.

For brevity, we shall refer to periodic state Φ as a *periodic orbit* if it satisfies

$$\Phi(z + R) = \Phi(z) \quad (65)$$

for any discrete translation $R = n_1 \mathbf{a}_1 + n_2 \mathbf{a}_2 \in \mathcal{L}$, where $\{n_1, n_2\}$ are any integers, and $(\mathbf{a}_1, \mathbf{a}_2)$ is a pair of \mathbb{Z}^2 integer lattice vectors that define a *primitive cell*. We shall

always refer to a Bravais sublattice (sublattice of \mathbb{Z}^2) by its unique Hermite normal form primitive cell (64) (basis?), and denote it $\mathcal{L} = [L \times T]_S$, a 2-dimensional doubly-periodic (relative) *periodic orbit*

$$\phi_{nt} = \phi_{n+L,t} = \phi_{n+S,t+T}, \quad (n,t) \in \mathbb{Z}^2 \quad (66)$$

with periods (L, T) and tilt S .

2020-03-17 Han In order to determine all prime tiles

$$\mathbf{b}_1 = \begin{pmatrix} L_p \\ 0 \end{pmatrix}, \quad \mathbf{b}_2 = \begin{pmatrix} S_p \\ T_p \end{pmatrix}, \quad (67)$$

that tile a larger tile

$$\mathbf{a}_1 = \begin{pmatrix} L \\ 0 \end{pmatrix}, \quad \mathbf{a}_2 = \begin{pmatrix} S \\ T \end{pmatrix}, \quad (68)$$

observe that a prime tile tiles the larger tile only if its width L is a multiple of L_p , its height T is a multiple of T_p , and the tile ‘tilts’ are related by

$$\mathbf{a}_2 = n\mathbf{b}_1 + \frac{T}{T_p}\mathbf{b}_2 \quad \rightarrow \quad S = nL_p + \frac{T}{T_p}S_p \quad (69)$$

i.e., the area spanned by the two ‘tilted’ primitive vectors $\mathbf{a}_2 \times \mathbf{b}_2 = ST_p - TS_p$ must be a multiple of the prime tile area L_pT_p .

Another way to understand the prime tile condition is illustrated in figure 1. The gray parallelogram is the primitive cell of the larger tile and the blue parallelogram is the primitive cell of the prime tile. In this figure we assume that the first two relations, L_p divides L and T_p divides T are already satisfied. In the periodic field over the larger tile, the field value at the tip of \mathbf{a}_2 (marked A) is the same as the field value at the origin O . And for the periodic field of the prime tile, the field value at the tip of $(T/T_p)\mathbf{b}_2$ (marked B) is same as the field value on the origin, hence the field values at points A and B are the same, $\mathbf{a}_2 = (T/T_p)\mathbf{b}_2$ which requires that $A - B$ can be divided by L_p . So $S - (T/T_p)S_p$ must be divisible by L_p .

2020-06-05 Han Suppose a Bravais lattice \mathcal{L} with basis

$$\mathbf{\Lambda} = \left[\mathbf{a}_1 \mid \mathbf{a}_2 \right] = \begin{bmatrix} a_{11} & a_{12} \\ a_{21} & a_{22} \end{bmatrix} \\ \det \mathcal{L} = a_{11}a_{22} - a_{12}a_{21}. \quad (70)$$

is tiled by a finer lattice \mathcal{L}_p with a basis

$$\mathbf{\Lambda}_p = \left[\mathbf{a}_1^p \mid \mathbf{a}_2^p \right] = \begin{bmatrix} a_{11}^p & a_{12}^p \\ a_{21}^p & a_{22}^p \end{bmatrix} \\ \det \mathcal{L}_p = a_{11}^p a_{22}^p - a_{12}^p a_{21}^p. \quad (71)$$

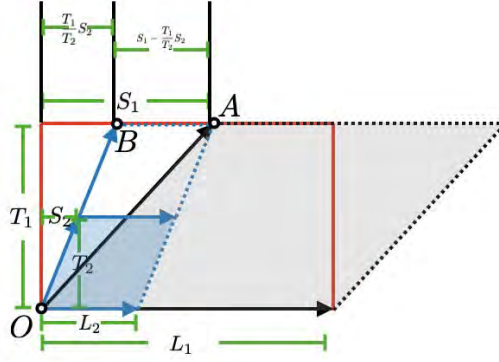


Figure 1: The gray parallelogram is the primitive cell of the large tile and the blue parallelogram is the primitive cell of the prime tile p , $T = 2T_p$ and $L = 3L_p$. The repeat the prime tile in the temporal direction reaches the upper boundary of the large tile at point B . If the prime tile can tile the large tile then the periodic boundary of the prime tile should satisfy the periodic boundary of the large tile. So the field value at point B should be same as the field value at point A . The distance between point B and point A should be equal to L_p multiplied by an integer.

As \mathcal{L} is a sublattice of \mathcal{L}_p , the basis must satisfy

$$\mathbf{\Lambda} = \left[k\mathbf{a}_1^p + l\mathbf{a}_2^p \mid m\mathbf{a}_1^p + n\mathbf{a}_2^p \right] = \mathbf{\Lambda}_p \begin{bmatrix} k & m \\ l & n \end{bmatrix}, \quad (72)$$

where k , l , m and n are integers. Solving this equation we have

$$\begin{aligned} k &= \frac{a_{11}a_{22}^p - a_{21}a_{12}^p}{\det \mathcal{L}_p}, & l &= \frac{a_{21}a_{11}^p - a_{11}a_{21}^p}{\det \mathcal{L}_p} \\ m &= \frac{a_{12}a_{22}^p - a_{22}a_{12}^p}{\det \mathcal{L}_p}, & n &= \frac{a_{22}a_{11}^p - a_{12}a_{21}^p}{\det \mathcal{L}_p}, \end{aligned} \quad (73)$$

and

$$\frac{\det \mathcal{L}}{\det \mathcal{L}_p} = \det \begin{bmatrix} k & m \\ l & n \end{bmatrix} = kn - lm. \quad (74)$$

To satisfy these relations, $|\mathbf{a}_1 \times \mathbf{a}_1^p|$, $|\mathbf{a}_1 \times \mathbf{a}_2^p|$, $|\mathbf{a}_2 \times \mathbf{a}_1^p|$ and $|\mathbf{a}_2 \times \mathbf{a}_2^p|$ need to be multiples of the prime tile area $\det \mathcal{L}_p$, with one relation on these integers imposed by the volume ratio (74) also being an integer.

2020-08-15 Predrag Is

$$\text{tr} \begin{bmatrix} k & m \\ l & n \end{bmatrix} = \text{tr} (\mathbf{\Lambda}_p^{-1} \mathbf{\Lambda}) \quad (75)$$

an important invariant?

2020-08-15 Predrag Any integer $[2 \times 2]$ matrix with nonvanishing determinant defines a primitive cell, so we can turn the above argument around. The form of (72)

suggests that if we have two prime lattices, we can construct a ‘non-prime’ (?) Bravais lattice by multiplication

$$\mathbf{\Lambda}_{pp'} = \mathbf{\Lambda}_p \mathbf{\Lambda}_{p'}. \quad (76)$$

Can we construct all Bravais lattices this way? Not clear, as the two primitive cells do not commute, $\mathbf{\Lambda}_p \mathbf{\Lambda}_{p'} \neq \mathbf{\Lambda}_{p'} \mathbf{\Lambda}_p$. Their volumes do multiply $\det \mathbf{\Lambda}_{pp'} = \det \mathbf{\Lambda}_p \det \mathbf{\Lambda}_{p'}$ so it is still possible they generate the same Bravais lattice, or two within an relative periodic orbit family of the same volume, but different tilt.

The ordered concatenations of primes, [ChaosBook Appendix A18.2 Prime factorization for dynamical itineraries](#) might do the trick.

See also the factorization algorithm (??).

2020-08-15 Predrag This checks with the Hermite normal form basis (67), where $a_{21} = a_{21}^p = 0$:

$$k = \frac{LT_p}{\det \mathcal{L}_p} = \frac{L}{L_p}, \quad l = 0,$$

$$m \det \mathcal{L}_p = ST_p - TS_p, \quad n = \frac{TL_p}{\det \mathcal{L}_p} = \frac{T}{T_p},$$

The volume relation

$$\frac{\det \mathcal{L}}{\det \mathcal{L}_p} = \det \begin{bmatrix} k & m \\ 0 & n \end{bmatrix} = kn \quad (77)$$

is trivially true. The trace (78)

$$\text{tr} \begin{bmatrix} k & m \\ l & n \end{bmatrix} = \frac{L}{L_p} + \frac{T}{T_p} \quad (78)$$

does not depend on S , so it is not an invariant that we are looking for.

2020-08-15 Predrag Consider now the prime primitive cell whose volume is a prime number,

$$\det \mathcal{L}_p = p.$$

Its only divisor is the unit cell of \mathbb{Z}^2 , so (73) becomes

$$\begin{bmatrix} k & m \\ l & n \end{bmatrix} = \begin{bmatrix} a_{11} & a_{12} \\ a_{21} & a_{22} \end{bmatrix}. \quad (79)$$

In the Hermite normal form basis (67) we chose $L = p$, $T = 1$, so

$$\begin{bmatrix} k & m \\ l & n \end{bmatrix} = \begin{bmatrix} L & S \\ 0 & T \end{bmatrix}, \quad S = 0, 1, \dots, p-1. \quad (80)$$

According to (73) the unimodular-transformation invariant formula (is it?) for S is

$$S = \mathbf{a}_2 \times \mathbf{a}_2^p = a_{12}a_{22}^p - a_{22}a_{12}^p, \quad (81)$$

where Λ_p is an unit area primitive cell (not necessarily the unit square) that tiles \mathcal{L} .

Some of discussion in the **2020-07-11 Predrag** post, around eq. (??), might be relevant.

2020-08-15 Predrag As an example of an arbitrary primitive cell Λ , consider the prime Bravais lattice figure ??, with the ‘integral basis’ vectors (??) and $\det \mathcal{L} = 7$

$$\begin{bmatrix} a_{11} & a_{12} \\ a_{21} & a_{22} \end{bmatrix} = \begin{bmatrix} 3 & 2 \\ 1 & 3 \end{bmatrix}. \quad (82)$$

7.3. Repeats of prime periodic states (failed attempt)

2023-06-08 Predrag Not sure this is the right file retiling.tex

2022-10-05 Predrag This section is WRONG IF probability of a repeat assumed in (85) is not multiplicative, as is the case for orbit Jacobian matrices, see (99). But (87) is a subsum, only the rectangles, no slants.

A field configuration $\Phi_{\mathbf{a}}$ occurs with probability density

$$P[\Phi_{\mathbf{a}}] = \frac{1}{Z_{\mathbf{a}}} e^{-S_{\mathbf{a}}[\Phi_{\mathbf{a}}]}, \quad Z_{\mathbf{a}} = Z_{\mathbf{a}}[0]. \quad (83)$$

Here $Z_{\mathbf{a}}$ is a normalization factor, given by the *partition sum*, the sum (in continuum, the integral) over probabilities of all configurations,

$$Z_{\mathbf{a}}[\mathbf{J}_{\mathbf{a}}] = e^{N_{\mathbf{a}}W_{\mathbf{a}}} = \int d\Phi_{\mathbf{a}} P[\Phi_{\mathbf{a}}] e^{\Phi_{\mathbf{a}} \cdot \mathbf{J}_{\mathbf{a}}}, \quad d\Phi_{\mathbf{a}} = \prod_z^{\mathbf{a}} d\phi_z, \quad (84)$$

where $\mathbf{J} = \{j_z\}$ is an external source j_z that one can vary site by site, and $S_{\mathbf{a}}[\Phi]$ is the action that defines the theory (discussed in more detail in section 11). The dimension of the partition function integral equals the number of lattice sites $N_{\mathbf{a}}$, i.e., the lattice volume (41).

A repeat of a *prime* primitive cell $\mathcal{L}_{\mathbf{a}}$ along direction a_1 is given by

$$Z_{\mathbf{a}}^2 = \int d\Phi_{\mathbf{a}} P[\Phi_{\mathbf{a}}] P[\Phi_{\mathbf{a}}] e^{2\Phi_{\mathbf{a}} \cdot \mathbf{J}_{\mathbf{a}}}. \quad (85)$$

Summing over all repeats we get

$$Z_{\mathbf{a}}[\mathbf{J}_{\mathbf{a}}; z_1] = \int d\Phi_{\mathbf{a}} \frac{P[\Phi_{\mathbf{a}}] z_1}{1 - P[\Phi_{\mathbf{a}}] z_1} = \int d\Phi_{\mathbf{a}} \frac{e^{N_{\mathbf{a}}W_{\mathbf{a}} z_1}}{1 - e^{N_{\mathbf{a}}W_{\mathbf{a}} z_1}}. \quad (86)$$

(fix up the notation!)

In the case of an Euclidean theory symmetric under all spacetime axes a_j interchanges, we need only one generating function variable, $z_j = z$. Carrying out the summation for a 2-dimensional spatiotemporal square lattice, we resum by summing first over the equal area (anti) diagonals $N_{\mathbf{a}} = L_{\mathbf{a}} + T_{\mathbf{a}}$, then over $N_{\mathbf{a}}$, obtaining

$$Z_{\mathbf{a}}[\mathbf{J}_{\mathbf{a}}; z] = \int d\Phi_{\mathbf{a}} \frac{P[\Phi_{\mathbf{a}}] z}{(1 - P[\Phi_{\mathbf{a}}] z)^2} = \int d\Phi_{\mathbf{a}} \frac{e^{N_{\mathbf{a}}W_{\mathbf{a}} z}}{(1 - e^{N_{\mathbf{a}}W_{\mathbf{a}} z})^2}. \quad (87)$$

(Now sum over all primes, do cumulant expansion (??), get cycle expansions for observables.)

7.4. Resolvent of W

We assume that the deterministic system under consideration is *uniformly hyperbolic*, i.e., that the stability eigen-exponents $\lambda_{c,\alpha} = \ln |\Lambda_{c,\alpha}|/N_c$ of every periodic state are finite and strictly bounded from above and below,

$$-\infty < \lambda_{min} \leq \lambda_{c,\alpha} \leq \lambda_{max} .$$

Hence every primitive cell partition sum is exponentially bounded,

$$\lambda_{min} \leq W_{\mathbb{A}}[0] \leq \lambda_{max} .$$

It is reasonable to suppose that there exist constants $M > 0$, $s_0 \geq 0$ such that

$$Z_{\mathbb{A}} = e^{tW_{\mathbb{A}}} \leq M e^{ts_0} \text{ for all } t \geq 0, \quad t = N_{\mathbb{A}}$$

What does that mean? We are assuming that no value of $e^{tW_{\mathbb{A}}}\rho(\phi)$ grows faster than exponentially for any choice of function $\rho(\phi)$, so that the fastest possible growth can be bounded by e^{ts_0} , a reasonable expectation in the light of the simplest example studied so far, the escape rate. If that is so, multiplying $e^{tW_{\mathbb{A}}}$ by e^{-ts_0} we construct a new operator $e^{-ts_0}e^{tW_{\mathbb{A}}} = e^{t(W-s_0I)}$ which decays exponentially for large t , $\|e^{t(W-s_0I)}\| \leq M$. We say that $e^{-ts_0}e^{tW_{\mathbb{A}}}$ is an element of a *bounded* semigroup with generator $W - s_0I$. Given this bound, it follows by the Laplace transform

$$\int_0^\infty dt e^{-st} e^{tW_{\mathbb{A}}} = \frac{1}{s - W}, \quad \Re s > s_0, \quad (88)$$

that the *resolvent* operator $(s - W)^{-1}$ is bounded

$$\left\| \frac{1}{s - W} \right\| \leq \int_0^\infty dt e^{-st} M e^{ts_0} = \frac{M}{s - s_0}. \quad (89)$$

If one is interested in the spectrum of \mathcal{L} , as we will be, the resolvent operator is a natural object to study; it has no Bravais lattice volume dependence, and it is bounded. It is clear that the leading eigenvalue $s_0(\beta)$ corresponds to the pole in (89).

The main lesson of this brief aside is that for continuous time flows, the Laplace transform is the tool that brings down the XXX in refeq3.16a into the resolvent form (88) and enables us to study its spectrum.

8. Orbit stability

The central insight of spatiotemporal field theory is the notion of *global* orbit stability. What we lack is the associated flow (analogue of the temporal Perron-Frobenius operator).

It might be the *Laplacian as a generator of diffusion* (??).

It might be the stability of *Newton descent*, page ??.

It might be *Gel'fand-Yaglom theorem's* 'Fredholm' operator, page ??.

For field theories considered here, the orbit Jacobian operators are of form

$$\mathcal{J}_{zz'} = -\square_{zz'} + V''(\phi_z) \delta_{zz'}, \quad (90)$$

with the free field ϕ^3 , ϕ^4 orbit Jacobian operators

$$\mathcal{J}_{zz'} = -\square_{zz'} + \mu^2 \delta_{zz'}, \quad (91)$$

$$\mathcal{J}_{zz'} = -\square_{zz'} - 2\mu^2 \phi_z \delta_{zz'}, \quad (92)$$

$$\mathcal{J}_{zz'} = -\square_{zz'} + \mu^2(1 - 3\phi_z^2) \delta_{zz'}. \quad (93)$$

Sometimes it is convenient to lump the diagonal terms of the discrete Laplace operator together with the site potential $V''(\phi_z)$. In that case, the orbit Jacobian operator takes the $2d + 1$ banded form

$$\mathcal{J} = \sum_{j=1}^d (-r_j + \mathcal{D} - r_j^{-1}), \quad \mathcal{D}_{zz'} = d_z \delta_{zz'}, \quad d_z = V''(\phi_z)/d + 2, \quad (94)$$

where r_j shift operators translate the field configuration by one lattice spacing in the j th hypercubic lattice direction, and we refer to d_z as the *stretching factor* at lattice site z . For the free field and spatiotemporal cat (91), ϕ^3 (172), ϕ^4 (190) theories the stretching factor d_z is, respectively,

$$s = \mu^2/d + 2, \quad (95)$$

$$d_z = -2\mu^2 \phi_z/d + 2, \quad (96)$$

$$d_z = \mu^2(1 - 3\phi_z^2)/d + 2. \quad (97)$$

In solid state physics operator (94) is known as the discrete Schrödinger operator [5, 47].

In what follows, it is crucial to distinguish the $[N_{\mathbb{A}} \times N_{\mathbb{A}}]$ orbit Jacobian matrix, evaluated over a finite volume primitive cell \mathbb{A} , from the orbit Jacobian operator (94) that acts on the infinite Bravais lattice $\mathcal{L}_{\mathbb{A}}$.

8.1. Primitive cell stability of a periodic state

Solutions of a nonlinear field theory are in general not translation invariant, so the orbit Jacobian matrix (47) (or the ‘discrete Schrödinger operator’ [5, 47])

$$\mathcal{J}_c = \begin{pmatrix} d_0 & -1 & 0 & 0 & \cdots & 0 & -1 \\ -1 & d_1 & -1 & 0 & \cdots & 0 & 0 \\ 0 & -1 & d_2 & -1 & \cdots & 0 & 0 \\ \vdots & \vdots & \vdots & \vdots & \ddots & \vdots & \vdots \\ 0 & 0 & 0 & 0 & \cdots & d_{n-2} & -1 \\ -1 & 0 & 0 & 0 & \cdots & -1 & d_{n-1} \end{pmatrix} \quad (98)$$

is not a circulant matrix: each periodic state Φ_c has its own orbit Jacobian matrix $\mathcal{J}_c = \mathcal{J}[\Phi_c]$, with the ‘stretching factor’ $d_t = V''(\phi_t) + 2$ at the lattice site t a function of the site field ϕ_t .

The orbit Jacobian matrix of a period- (mn) periodic state Φ , which is a m -th repeat of a period- n prime periodic state Φ_p , has a tri-diagonal block circulant matrix form

that follows by inspection from (98):

$$\mathcal{J}_{p^r} = \begin{pmatrix} \mathbf{s}_p & -\mathbf{r} & & -\mathbf{r}^\top \\ -\mathbf{r}^\top & \mathbf{s}_p & -\mathbf{r} & \\ & \ddots & \ddots & \ddots \\ & & -\mathbf{r}^\top & \mathbf{s}_p & -\mathbf{r} \\ -\mathbf{r} & & & -\mathbf{r}^\top & \mathbf{s}_p \end{pmatrix}, \quad (99)$$

where block matrix \mathbf{s}_p is a $[n \times n]$ symmetric Toeplitz matrix

$$\mathbf{s}_p = \begin{pmatrix} d_0 & -1 & & 0 \\ -1 & d_1 & -1 & \\ & \ddots & \ddots & \ddots \\ & & -1 & d_{n-2} & -1 \\ 0 & & & -1 & d_{n-1} \end{pmatrix}, \quad \mathbf{r} = \begin{pmatrix} 0 & \cdots & 0 \\ & \ddots & \vdots \\ 1 & & 0 \end{pmatrix}, \quad (100)$$

and \mathbf{r} and its transpose enforce the periodic bc's. This period- (mn) periodic state Φ orbit Jacobian matrix is as translation-invariant as the temporal cat, but now under Bravais lattice translations by multiples of n . One can visualize this periodic state as a tiling of the integer lattice \mathbb{Z} by a generic periodic state field decorating a tile of length n . The orbit Jacobian matrix \mathcal{J} is now a block circulant matrix which can be brought into a block diagonal form by a unitary transformation, with a repeating $[n \times n]$ block along the diagonal.

9. Orbit Jacobian matrices as block matrices

By reshaping the d -dimensional periodic states as vectors the tensors, the multi-index orbit Jacobian matrices \mathcal{J} can be rewritten as block matrices. For example consider a $[L \times T]_0$ periodic state Φ_c of a two-dimensional spatiotemporal ϕ^4 theory (12). Reshape the spatiotemporal periodic state as a temporal periodic state with the spatial dependence treated as a multicomponent field at each temporal lattice site. Then the orbit Jacobian matrix is a $[T \times T]$ block matrix,

$$\mathcal{J}_A = \begin{pmatrix} \mathbf{s}_0 & -\mathbb{1} & & -\mathbb{1} \\ -\mathbb{1} & \mathbf{s}_1 & -\mathbb{1} & \\ & \ddots & \ddots & \ddots \\ & & -\mathbb{1} & \mathbf{s}_{T-2} & -\mathbb{1} \\ -\mathbb{1} & & & -\mathbb{1} & \mathbf{s}_{T-1} \end{pmatrix}, \quad (101)$$

with $[L \times L]$ matrix block \mathbf{s}_t

$$\mathbf{s}_t = \begin{pmatrix} d_{0,t} & -1 & & -1 \\ -1 & d_{1,t} & -1 & \\ & \ddots & \ddots & \ddots \\ & & -1 & d_{L-2,t} & -1 \\ -1 & & & -1 & d_{L-1,t} \end{pmatrix}, \quad (102)$$

and $\mathbb{1}$ a $[L \times L]$ identity matrix. For a periodic state with periodicity $[L \times T]_S$ the orbit Jacobian matrix is still a tri-diagonal block matrix, but with relative periodic boundary conditions, imposed by the non-zero shift S :

$$\mathcal{J} = \begin{pmatrix} \mathbf{s}_0 & -\mathbb{1} & & & -r_1^S \\ -\mathbb{1} & \mathbf{s}_1 & -\mathbb{1} & & \\ & \ddots & \ddots & \ddots & \\ & & & -\mathbb{1} & \mathbf{s}_{T-2} & -\mathbb{1} \\ -r_1^S & & & & -\mathbb{1} & \mathbf{s}_{T-1} \end{pmatrix}, \quad (103)$$

where r_1 is a $[L \times L]$ cyclic shift matrix $(r_1)_{n,n'} = \delta_{n+1,n'}$.

A spatiotemporal lattice field theory which couples adjacent field values by discrete Laplace operator (127) has orbit Jacobian matrices with tri-diagonal form similar to (101). For example, a $[L \times T]_0$ periodic state of a uniform stretching systems such as the two-dimensional spatiotemporal cat (10) has orbit Jacobian matrix (101)–(102) but $s_{l,t}$ is a constant $2s$ that does not depend on the field values at each lattice site. The spatiotemporal-translation invariance allows one to compute the eigenvalues of the orbit Jacobian matrix using the discrete Fourier transform.

10. Observables

2022-01-19, 2023-02-11 Predrag Because of the dependence of the orbit Jacobian matrix (99) on the primitive cell \mathbf{A} repeat number r , we have to distinguish the partition function $Z_{\mathbf{A}}$ defined over the finite lattice volume $N_{\mathcal{L}} = N_{\mathbf{A}}$ primitive cell from the (infinite) lattice partition function $Z_{\mathcal{L}}$, which is the sum over all distinct primitive cells.

A field configuration Φ over a primitive cell \mathbf{A} of lattice \mathcal{L} occurs with probability density

$$P_{\mathbf{A}}[\Phi] = \frac{1}{Z} e^{-S_{\mathbf{A}}[\Phi]}, \quad Z = Z_{\mathcal{L}}[0]. \quad (104)$$

Here $Z_{\mathcal{L}}$ is a normalization factor, given by the *partition sum*, the sum (in continuum, the integral) over probabilities of all configurations,

$$Z_{\mathcal{L}}[J] = e^{N_{\mathcal{L}}W_{\mathcal{L}}} = \int_{\mathcal{L}} d\Phi P[\Phi] e^{\Phi \cdot J}, \quad d\Phi = \prod_z^{\mathcal{L}} d\phi_z, \quad (105)$$

where $J = \{j_z\}$ is an external source j_z that one can vary site by site, and $S[\Phi]$ is the action that defines the theory (discussed in more detail in section 11). The dimension of the partition function integral equals the number of lattice sites $N_{\mathcal{L}}$, i.e., the lattice volume (41).

Birkhoff sum [30] over primitive cell c

$$A_c = \sum_{z \in c} a_z. \quad (106)$$

Birkhoff average over primitive cell c

$$\langle a \rangle_c = \frac{A_c}{N_c}. \quad (107)$$

The free energy (the large-deviation potential?)

$$\begin{aligned} Z_{\mathbf{A}}[0] &= \sum_c e^{N_{\mathcal{L}} W_c[0]} \\ e^{N_{\mathcal{L}} W_c[0]} &= \int_{\mathcal{M}_c} d\Phi \delta(F[\Phi]) = \frac{1}{|\text{Det } \mathcal{J}_c|} \end{aligned} \quad (108)$$

was originally snuck into (15) (see (??), (??), (??)) See also partition function (??), (??), (??); partition sum (??); Gaussian (??); Ising (??).

10.1. Birkhoff sums

2022-04-17 Predrag In number theory, probability theory and dynamical systems literature the integrated observable is sometimes called a ‘Birkhoff sum’, and the time average along an orbit is sometimes called a ‘Birkhoff average’.

What I (used to) call in ChaosBook the ‘integrated observable’ mathematicians (sometimes?) call the ‘Birkhoff sum’,

$$A_k = \sum_{j=1}^k a_j \quad (109)$$

and the time average along an orbit is sometimes called a ‘Birkhoff average’. See Oliver Knill *Birkhoff sum*.

see [ChaosBook Appendix: Averaging](#)

see [ChaosBook Remark A20.1. Cumulants](#)

10.2. Reject rate

ChaosBook: “Local quantities, such as the eigenvalues of equilibria and periodic orbits and global quantities, such as Lyapunov exponents, metric entropy, and fractal dimensions, are examples of dynamical system properties that are independent of coordinate choice.”

2024-07-02 Predrag and Han In dynamical systems theory, for open systems the rate at which trajectories leave the system per unit time is called *escape rate*, see [ChaosBook eq. \(1.3\)](#),

2024-07-02 Predrag For the relation between stability exponent λ , metric entropy h and escape rate γ , see [ChaosBook eq. \(22.11\)](#).

10.3. Expectation values, à la Josh & Sam

From CL18:

For a given \mathcal{L}_p -periodic prime periodic state Φ_p , the *Birkhoff average* of observable $a[\Phi]_z$ is given by the Birkhoff sum A_p ,

$$\langle a \rangle_p = \frac{1}{N_p} A_p, \quad A_p = \sum_{z \in \mathbb{A}_p} a[\Phi_p]_z. \quad (110)$$

$$Z_{\mathbb{A}}[\beta] = \sum_c \int_{\mathcal{M}_c} d\Phi_{\mathbb{A}} \delta(F[\Phi]) e^{N_{\mathbb{A}}\beta \cdot a_{\mathbb{A}}[\Phi]} = \sum_c \frac{1}{|\text{Det } \mathcal{J}_c|} e^{N_{\mathbb{A}}\beta \cdot \langle a \rangle_c}, \quad (111)$$

$$Z_{\mathbb{A}}[\beta] = \sum_c Z_c, \quad Z_c = e^{N_{\mathbb{A}}(\beta \cdot \langle a \rangle_c - \lambda_c)}, \quad (112)$$

The orbit Jacobian operator of a periodic state Φ_c :

$$(\mathcal{J}_c)_{zz'} = \frac{\delta F[\Phi_c]_z}{\delta \phi_{z'}}, \quad z \in \mathbb{Z}^d, \quad (113)$$

and its determinant, the *Hill determinant* $\text{Det } \mathcal{J}_c$.

The stabilities of periodic states can be evaluated using either the orbit Jacobian matrix (113), a high-dimensional matrix computed globally over the periodic state, or the forward-in-time Floquet matrix \mathbb{J}_c , a low-dimensional matrix computed at a given periodic state time instant. The two ways of computing stability are related by the *Hill's formula*:

$$|\text{Det } \mathcal{J}_c| = |\det(\mathbf{1} - \mathbb{J}_c)|. \quad (114)$$

In the companion paper I [32] we derive the Hill's formula for temporal systems. The derivation of Hill's formula for spatiotemporal systems is similar.

For a one-dimensional, temporal Bravais lattice, the generating function of the deterministic partition function (112) is known as the deterministic trace formula (see [ChaosBook eq. \(21.24\)](#)), see (122) As here every periodic state weight contributes with a positive sign, there are no cancelations, and the key property of hyperbolic flow trajectories, that they are shadowed by shorter trajectories, is here not taken into account. That is accomplished by reorganizing the periodic state contributions into the dynamical zeta function [45] (116).

Our spatiotemporal zeta function - a two-dimensional generalization of the dynamical zeta function (116) - is related to the deterministic generating partition function (two-dimensional generalization of the deterministic trace formula (122)) by the usual logarithmic derivative relation between the partition sum and the zeta function

$$Z[\beta, z] = z \frac{d}{dz} \ln \zeta[\beta, z] = \sum_p N_p \sum_{n=1}^{\infty} \frac{nt_p^n}{1 - t_p^n}, \quad (115)$$

see, for example, [ChaosBook eq. \(18.24\)](#).

From (110):

$$N_p \langle a \rangle_p = \sum_{z \in \mathbb{A}_p} a_z.$$

From (111), (112):

$$W[\beta] = \ln \sum_p N_p Z_p[\beta], \quad Z_p[\beta] = e^{W_p[\beta]}$$

$$\left. \frac{\partial}{\partial \beta} W[\beta] \right|_{\beta=0} = \frac{1}{Z[0]} \sum_p N_p Z_p[0] \left. \frac{\partial W_p[\beta]}{\partial \beta} \right|_{\beta=0}. \quad Z_p[0] = \frac{N_p}{|\text{Det} \mathcal{J}_p|}$$

For a 1-dimensional, temporal lattice (122), this agrees with Josh & Sam (maybe I did not get all N_p right.

[... the above is TO BE REWRITTEN]

2023-02-10, 2024-03-31, 2024-04-13 Han and Predrag's derivation of Josh & Sam's prime orbits expectation value formula (120), as given in the current draft of Joshua L. Pughe-Sanford, Sam Quinn, Teodor Balabanski, and Roman O. Grigoriev *Computing chaotic time-averages from a small number of periodic orbits* (2024). Start with the Euler product form of the dynamical zeta function [45],

$$1/\zeta = \prod_p (1 - t_p) \quad (116)$$

$$t_p = \frac{1}{|\Lambda_p|} e^{T_p(\beta\langle a \rangle_p - s)}, \quad z = e^{-s}. \quad (117)$$

In **ChaosBook** eq. (23.25), the cycle averaging formula

$$\langle a \rangle = \langle A \rangle_\zeta / \langle T \rangle_\zeta = - \left. \frac{\partial}{\partial \beta} \frac{1}{\zeta} \right|_{\beta=0, s=s_0} / \left. \frac{\partial}{\partial s} \frac{1}{\zeta} \right|_{\beta=0, s=s_0}$$

is evaluated ordered by increasing pseudocycle periods,

$$\langle A \rangle_\zeta = \sum' A_\pi t_\pi \langle T \rangle_\zeta = \sum' T_\pi t_\pi, \quad (118)$$

with the 'escape rate' $= -s_0$ in the weight t_p determined by the leading zero of the dynamical zeta function (116).

Josh & Sam take instead the derivative of each term $(1 - t_p)$ in the formal product (116), for a confined, probability conserving $s_0 = 0$ escape rate, resulting in the cute but troubled

$$\left. \frac{\partial}{\partial \beta} 1/\zeta \right|_{\beta=0} = -1/\zeta \sum_p \frac{1}{1 - t_p} \left. \frac{\partial t_p}{\partial \beta} \right|_{\beta=0}, \quad \frac{\partial t_p}{\partial \beta} = A_p t_p. \quad (119)$$

Prior to 0/0 setting $s = 0$, the overall $-1/\zeta$'s factors cancel, resulting in Josh & Sam's über-simple probability P_p of prime orbit p weighted formula

$$\langle a \rangle = \sum_p P_p \langle a \rangle_p, \quad P_p = \frac{T_p / (|\Lambda_p| - 1)}{\sum_{p'} T_{p'} / (|\Lambda_{p'}| - 1)}. \quad (120)$$

What's not nice about it, is that it is not ordered by increasing z^N .

Proposal: cut off the z power series at the period $T = T_{p'}$ of the longest prime p' included, keep the p repeat terms in the geometric series expansion of $1/(1 - t_p)$

only up to $rT_p \leq T$. Exponential convergence. No pseudocycles, so no shadowing. Plot $\langle a \rangle_T$. It might be OK.

Various way of seeing (120) is not nice. The simplest, I think, is [ChaosBook sect 22.4 False zeros](#). Or, as Han explains below, due to [ChaosBook sect 23.4 Flow conservation sum rules](#), both the expectation value and mean period series are divergent at $s = s_0$ escape rate, where we are using them.

2024-03-31 Han The numerator, denominator of (118) are

$$-\frac{\partial}{\partial \beta} \ln(1/\zeta) \Big|_{\beta=0, s=s_0} = \sum_p \frac{T_p \langle a \rangle t_p}{1 - t_p} \Big|_{\beta=0, s=s_0} = \sum_p \frac{T_p \langle a \rangle}{|\Lambda_p| - 1},$$

$$\frac{\partial}{\partial s} \ln(1/\zeta) \Big|_{\beta=0, s=s_0} = \sum_p \frac{T_p t_p}{1 - t_p} \Big|_{\beta=0, s=s_0} = \sum_p \frac{T_p}{|\Lambda_p| - 1},$$

specializing to bound systems' $s_0 = 0$ in the third terms.

In Josh & Sam's formula (120), the denominator increases linearly as more prime orbits are included, since for prime orbits with period T :

$$\lim_{T \rightarrow \infty} \sum_{p: T_p=T} \frac{T_p}{|\Lambda_p| - 1} = \lim_{T \rightarrow \infty} \sum_{p: T_p=T} \frac{T_p}{|\Lambda_p|} = 1 \quad (121)$$

for a bound system. If a system is not bound, add a $e^{\gamma T_p}$ factor to every T_p so the exponential increase of number of prime orbits and exponential decrease of weight sum balance out, and the relation (121) still holds.

Our generating function (ChaosBook deterministic trace formula)

$$Z[\beta, z] = \sum_p Z_p[\beta, z]$$

$$Z_p[\beta, z] = N_p \sum_{r=1}^{\infty} t_p^r = \frac{N_p t_p}{1 - t_p}, \quad (122)$$

with the primitive cell volume $N_p = T_p$ equal to the time period of a prime orbit of temporal evolution equation $\phi_{t+1} - f(\phi_t) = 0$ is similar to the numerator of (120), but I have not yet used its relation to the zeta function in order to actually compute this numerator. The derivative of the trace formula with respect to β is:

$$\frac{\partial}{\partial \beta} Z[\beta, z] \Big|_{z=1, \beta=0} = \sum_p \frac{T_p^2 \langle a \rangle_p}{|\Lambda_p| - 1} + ?$$

There is an extra T_p because the numerator of (120) is proportional to $\frac{\partial}{\partial \beta} \zeta$, while using (115) our computation of the partition function is:

$$\frac{\partial}{\partial \beta} Z[\beta, z] = z \frac{\partial^2}{\partial \beta \partial z} \ln \zeta.$$

The extra $\partial/\partial z$ brings out one more T_p .

2022-02-13 Josh & Sam Questions about how to best (and practically) evaluate cycle averaging formulas:

- (i) The numbers of terms in the expansion grows so quickly with respect to the minimal symbol length orbit excluded that we are not quite sure how and where to truncate the sum, even moderately sized collections of orbits.
- (ii) Has anyone attempted to compute periodic orbits averages by numerically computing the zero and derivative of $F = \prod_p (1 - t_p)$ directly?

2022-02-11 Predrag .

- (i) Nobody so far has had enough understanding of Navier-Stokes periodic orbits to evaluate truncation errors. For low-dimensional systems:
 - (a) If grammar is known, exponentially decreasing errors kick in only after ‘fundamental’ cycles are accounted for, read the end of [ChaosBook sect. 18.3 Determinant of a graph](#)
 - (b) If symbolic dynamics is not understood, [ChaosBook sect. 23.7 Stability ordering of cycle expansions](#)
- (ii) None has attempted it - an idea worth exploring.
 - (a) Watch out for [ChaosBook sect. 22.4 False zeros](#): the unexpanded product $\prod_p (1 - t_p)$ is only a shorthand, just like for the original Riemann zeta function.
 - (b) If you expand the terms as a (pseudo)cycle expansion, numerically “computing the zero and derivative” seems to be what we already do?
- (iii) But your question does lead to something that Matt Gudorf never explored in his thesis: Perhaps the most important insight of the spatiotemporal reformulation of ‘chaos’ is that the weight of periodic orbits (N -torus, if theory has N continuous symmetries) is given by its Hill determinant, see [LC21 sect 8.2 Periodic orbit theory for the retarded](#).
 - (a) Can you think of new/better ways to evaluate $\text{Det } \mathcal{J}$? Orbit Jacobian matrix \mathcal{J} is big, but very sparse, and $\text{Det } \mathcal{J}$ has a nice geometrical interpretation as a [LC21 fundamental parallelepiped](#)? The edges of the parallelepiped are the columns of the orbit Jacobian matrix, which are sparse, so maybe it is computable?
 - (b) In the continuum limit (more appropriate to Navier-Stokes?), maybe the best was is to follow [LC21 Hill and Poincaré](#) , and truncate Fourier series?
 - (c) For viscous flows, like Navier-Stokes, the infinity of transient, strongly dissipative modes immediately damp put, so the Hill determinant should only have the dimension of the *inertial manifold*. Does it?

11. Nonlinear lattice field theory

Consider a continuum scalar, one-component field, d -dimensional Euclidean ϕ^k theory defined by action [28, 42, 53]

$$S[\Phi] = \int d^d x \left\{ \frac{1}{2} [\partial_\mu \phi(x)]^2 + \frac{\mu^2}{2} \phi^2(x) - \frac{g}{k!} \phi^k(x) \right\}, \quad (123)$$

with the Klein-Gordon mass $\mu \geq 0$, and the strength of the self-coupling $g \geq 0$. Note the inverted potential - we are interested in unstable periodic states. 

The discretized ϕ^k theory [39] is defined as the lattice sum over the Euclidean Lagrangian density

$$S[\Phi] = \sum_z \left\{ \frac{1}{2} \sum_{\mu=1}^d (\partial_\mu \phi)_z^2 + \frac{\mu^2}{2} \phi_z^2 - \frac{g}{k!} \phi_z^k \right\}, \quad (124)$$

where we set lattice constant $a = 1$ throughout. In the spirit of anti-integrability [3], we split the action into ‘kinetic’ and the local ‘potential’ parts $S[\Phi] = -\frac{1}{2} \Phi^\top \square \Phi + V[\Phi]$, where the nonlinear self-interaction part is

$$V[\Phi] = \sum_z V(\phi_z), \quad V(\phi) = \frac{1}{2} \mu^2 \phi^2 - \frac{g}{k!} \phi^k, \quad k \geq 3 \quad (125)$$

with $V(\phi_z)$ a nonlinear potential, intrinsic to the lattice site z . The part bilinear in fields is the free field theory action

$$S_0[\Phi] = \frac{1}{2} \Phi^\top (-\square + \mu^2 \mathbf{1}) \Phi, \quad (126)$$

Here the lattice Laplacian

$$\square \phi_z = \sum_{\|z'-z\|=1} (\phi_{z'} - \phi_z) = \sum_{\|z'-z\|=1} \phi_{z'} - 2d \phi_z \quad \text{for all } z, z' \in \mathcal{L} \quad (127)$$

is the average of the lattice field variation $\phi_{z'} - \phi_z$ over the sites nearest to the site z . For a hypercubic lattice in one and two dimensions this discretized Laplacian is given by

$$\square \phi_t = \phi_{t+1} - 2\phi_t + \phi_{t-1} \quad (128)$$

$$\square \phi_{jt} = \phi_{j,t+1} + \phi_{j+1,t} - 4\phi_{jt} + \phi_{j,t-1} + \phi_{j-1,t}. \quad (129)$$

Discretizing $\partial/\partial t$ as the backward partial difference operator,

$$\frac{\partial \phi(t)}{\partial t} = \frac{\phi_t - \phi_{t-1}}{\Delta t}, \quad (130)$$

setting $\Delta t = 1$, the discretized Hamilton’s equations take form

$$\begin{aligned} \phi_{t+1} - \phi_t &= p_{t+1}, \\ p_{t+1} - p_t &= -V'(\phi_t), \end{aligned} \quad (131)$$

To go to the Lagrangian formulation, replace the momentum by the discretized velocity $p_t = \phi_t - \phi_{t-1}$,

$$\phi_{t+1} - \phi_t = \phi_t - \phi_{t-1} - V'(\phi_t).$$

For the discrete scalar field theory (124) the Euler–Lagrange equations take form of a 3-term recurrence (second-order difference equation)

$$\square \phi_z + V'(\phi)_z = 0. \quad (132)$$

Seen from the perspective of conventional scalar field theory, we are interested in the “lattice formulation, broken-symmetry phase” or the “Goldstone phase” setting. By “spontaneous breaking of the symmetry” in ϕ^4 theory one means that a solution does not satisfy $\phi \rightarrow -\phi$. That is obvious for our spatiotemporal chaotic, “turbulent” solutions. We work “beyond perturbation theory”, as we start out in the anti-integrable, strong coupling regime, in contrast to much of the literature that often studies weak coupling expansions around one of the minima.

12. Internal symmetries

In addition to spacetime ‘geometrical’ symmetries: invariance of the shape of a periodic state under coordinate translations, rotations, and reflections, a field theory might have *internal* symmetries, groups of transformations that leave the Euler–Lagrange equations invariant, but act only on a lattice site *field*, not on site’s location in the spacetime lattice.

Consider a general transformation of lattice field, $\phi_z \rightarrow g(\phi_z)$. The new Euler–Lagrange equation $F_z[g(\phi_z)]$ will be equivalent, but different in form. In that case, we need a convention to pick a particular form of the equation.

For example, under field inversion, $\phi \rightarrow -\phi$, the orbit (the set of all actions g) of temporal Hénon (or ϕ^3 theory) consists of two distinct but equivalent Euler–Lagrange equations, differing in the sign of the stretching coefficient a in (??). In contrast, the potential of the ϕ^4 theory is invariant under field inversion. In such case, where potential is invarinat under all transformations $g \in G$, all Euler–Lagrange equations in the group orbit of G are of the same form.

A theory has an internal symmetry, if the defining equation of the system is invariant under some transformations of the fields, without reference to their spacetime location. It maps solutions to equivalent solutions.

For example, the temporal Bernoulli (??) and the temporal cat (??) (but not the temporal Hénon) have an internal D_1 symmetry. The Euler–Lagrange equations of the temporal Bernoulli and the temporal cat are invariant under order-2 dihedral group D_1 inversion of the fields though the center of the $0 \leq \phi_z < 1$ unit interval,

$$\bar{\phi}_z = 1 - \phi_z \pmod{1}, \quad \text{for all } j \in \mathcal{L}, \quad (133)$$

and the corresponding inversion of lattice site symbol m_z .

For the temporal catwith a given integer stretching parameter s the alphabet ranges over $|\mathcal{A}| = s+1$ possible values for m_t ,

$$\mathcal{A} = \{\underline{1}, 0, \dots, s-1\}, \quad (134)$$

necessary to keep ϕ_t for all times t within the unit interval $[0, 1)$.

Inspection of the temporal cat figure ?? suggests that there is an internal symmetry under inversion though the center of the $0 \leq \phi_z < 1$ unit interval. Indeed, if $\mathbf{M} = \{m_{nt}\}$, composed of symbols from a given alphabet, corresponds to a 2-dimensional lattice state $\Phi_{\mathbf{M}} = \{\phi_{nt}\}$, its internal symmetry partner

$$\bar{\mathbf{M}} = \{\bar{m}_{nt}\}, \quad \bar{m}_{nt} = 2(s-2) - m_{nt}, \quad (135)$$

corresponds to lattice state $\bar{\Phi}_{\bar{\mathbf{M}}} = \{1 - \phi_{nt}\}$.

If $\Phi = \{\phi_z\}$ is a periodic state of the system, the inversion $\bar{\Phi} = \{\bar{\phi}_z\}$ is also an admissible periodic state. So, every periodic state of the temporal Bernoulli and the temporal cat either belongs to a pair of asymmetric periodic states $\{\Phi, \bar{\Phi}\}$, or is symmetric (self-dual) under the inversion.

See also section ?? *Internal symmetry factorization* and section ?? *Internal symmetry blog*.

2024-11-09 Predrag Quotient the internal D_1 symmetry for ϕ^4 , as in [ChaosBook fig. 11.5](#).

2021-07-17 Predrag to Han, Xaunqi and Sidney Looking at figure ??: The temporal cat (but not the temporal Hénon) has a *internal symmetry* under the simultaneous inversion S through the center of the $0 \leq \phi_j < 1$ unit interval, see (133). Can you check whether the (??), (??) Isola zeta function factorization is a consequence of this dynamical inversion symmetry? $S^2 = 1$ should give you the projection operators.

13. Dynamics in state space

Before discussing global properties for non-linear systems, it is conventional to take a dynamical point of view and start with local forward-in-time formulation in state space. Later this notion of local will be connected with a global picture.

Field theory is closely related with the study of dynamical system. However, such connection is not always clearly illustrated. Thus, a rigorous and detailed discussion of underlying mathematics is favorable here.

13.1. Preliminary definitions

To conform with tradition in dynamical system, let \mathcal{M} be state space that contains all possible field values, and $f : \mathcal{M} \times \mathcal{M} \rightarrow \mathcal{M}$ a self-homeomorphism on \mathcal{M} is corresponding discrete time evolution operator that satisfies semi-group property of time evolution, which is defined inductively

$$\begin{aligned} f^n &= f \circ f^{n-1} \\ f^0 &= id_{\mathcal{M}}. \end{aligned}$$

In such a system (\mathcal{M}, f) , an invariant subset $A \subset \mathcal{M}$ is a set such that

$$f(A) = A \quad (136)$$

Examples of invariant subset are fixed points, limit cycles (as periodic orbits), ω -limits, etc. These invariant subsets has drawn great attention in the study of complicated dynamical systems. Among them, the most helpful ones are stable (unstable) manifolds, which are defined based on fixed points,

$$\begin{aligned} W^s(f, p) &= \{q \in \mathcal{M} | f^n(q) = p, n \rightarrow \infty\} \\ W^u(f, p) &= \{q \in \mathcal{M} | f^{-n}(q) = p, n \rightarrow \infty\}, \end{aligned}$$

where superscripts s and u indicates stable and unstable respectively. In other words, stable/unstable manifolds are points attracted or repelled by the fixed point p . Anastassiou *et al* [1] used parameterization method to visualize stable/unstable manifolds for ϕ^4 theory and calculated homoclinic tangency. Locally near fixed points, the stable/unstable manifolds are locally straightened near fixed points with slopes determined by eigenvectors of Jacobian matrix (which is very reasonable as they agree in the tangent space at fixed points).

As introduced by Birkhoff[??] to strictly define dissipative systems, non-wandering set has been another important invariant subset in open systems where some solutions 'escape' from \mathcal{M} and never return. The non-wandering set is defined as the complement of wandering set [**<empty citation>**]. A point $x_0 \in \mathcal{M}$ is wandering if there exists a positive integer $N \in \mathbb{N}$ such that

$$\exists U \ni x_0, f^n(U) \cap U = \emptyset \forall n > N \tag{137}$$

which means that after finitely many iterations, this neighborhood of x is never visited by this given solution anymore (similar to transitive solution in Markov process). Thus, the wandering set \mathcal{W} is defined as

$$\mathcal{W} = \{x \in \mathcal{M} | x \text{ is wandering} \} \tag{138}$$

Correspondingly, the non-wandering set can be defined as $\mathcal{N} = \mathcal{M} \setminus \mathcal{W}$. In fact, non-wandering set of an open system is usually extremely complicated as zero-measure fractal with empty interior [11]. However, a finite-level rough visualization is available by the idea of Smale's horseshoe map. The usual practice is to take a large enough square cover near origin and map it forward and backward in time to intersect itself. Nevertheless, this practice seems rather artificial, since a square is in no way natural to the dynamics. A better approach is the find cover that is bounded by invariant manifolds instead (referred to as optimal cover later). This method is demonstrated using example of ϕ^3 and ϕ^4 in the following section.

In strong coupling regime, many physically important systems are characterized mathematically by Axiom A, which satisfies:

- (i) $\Omega(f)$ is compact
- (ii) The set of periodic point is dense in $\Omega(f)$

For any surface, hyperbolicity of non-wandering implies density, thus sometimes hyperbolic and axiom A are used interchangeably. The density of Axiom A

diffeomorphism ensures that there exists an open neighborhood of $U \supset \Omega(f)$ and

$$\Omega(f) = \bigcap_{z \in \mathbb{Z}} f^z(U) \quad (139)$$

is a locally maximal invariant set for f . This is important for visualization technique of non-wandering set. An Axiom A diffeomorphism also supports a Markov partition [6] that lays basis for definition of symbolic dynamics.

As another important dynamical concept, hyperbolicity is characterized by local properties of tangent bundle. A differentiable map f is said to have hyperbolic structure on subset $\Lambda \subset \mathcal{M}$ if its tangent space can be decomposed into a direct sum of contracting and expanding directions at every point in Λ . Formally, Λ is a hyperbolic set if $\forall x \in \Lambda$,

$$\begin{aligned} (i) \quad & T_x M = E_x^s \oplus E_x^u \\ (ii) \quad & d_x f(E_x^{s,u}) = E_{f(x)}^{s,u} \\ (iii) \quad & |d_x f|_{E_x^s} < \lambda_1, \quad |d_x f^{-1}|_{E_x^u} < 1/\lambda_2, \quad (0 < \lambda_1 < 1 < \lambda_2), \end{aligned}$$

which means that $E_x^{s,u}$ are subspaces that are invariant under differential of f and represent contraction and expansion respectively.

13.2. Dynamical formulation on non-linear field theories

Such formal discussion of dynamical systems would be meaningless if we cannot associate the non-linear field theories of interest a dynamical formulation. Indeed, it is as natural as the transition from Lagrangian to Hamiltonian for any field theories at hand. Limiting ourselves on the highly nontrivial one-dimensional deterministic field theories, state space is $\mathcal{M} = \mathbb{R}^2$ due to three-term recurrence relation of ϕ^3 and ϕ^4 (ref). Any point (represent a unique orbit) in \mathcal{M} can be thought as given by it initial conditions (ϕ_0, ϕ_1) or (ϕ_0, φ_0) where $\varphi_t = \phi_{t+1}$. Time evolution is given by field equation $\phi_{t+1} = g(\phi_t, \phi_{t-1})$, written in vector form as

$$\hat{f}(\hat{\phi}_t) = \hat{f}(\varphi)_t \quad \phi_t = (\phi)_t \quad g(\phi_t, \varphi_t) = (\phi)_t \quad \phi_{t+1} = \hat{\phi}_{t+1} \quad (140)$$

This operator \hat{f} is completely specified by $g : \mathbb{R}^2 \rightarrow \mathbb{R}$, and for ϕ^3 and ϕ^4 it is given by

$$\begin{aligned} g(\phi_t, \phi_{t-1}) &= -\phi_{t-1} + \mu^2(-1/4 + \phi_t^2) + 2\phi_t \quad (\phi^3) \\ g(\phi_t, \phi_{t-1}) &= -\phi_{t-1} - \mu^2\phi_t^3 + (\mu^2 + 2)\phi_t \quad (\phi^4) \end{aligned} \quad (141)$$

This dynamical formulation gives a way to look at local properties like Jacobian matrix \mathbb{J} or to inspect conditions for hyperbolicity in non-linear field theories. As temporal ϕ^3 theory is conjugate to the famous Henon map, studies on sufficient condition of hyperbolicity had been rich, and we just take result $a > 5.699310786700\dots$, which correspond to $\mu^2 > 5.17661\dots$. This makes us take $\mu^2 = 5.5$ for the rest discussion on ϕ^3 theory. In case of ϕ^4 theory, although it has attracted much attention in quantum field theory, the dynamical counterpart of ϕ^4 theory (which is a cubic map) is not as well

investigated as Hénon, but a lot of efforts has been devoted to find a lower bound, similar to the bound of parameter a given. We adopt criterion from (ref) and take $\mu^2 = 3.5$ for our discussion on ϕ^4 theory, whose hyperbolicity can also be shown graphically in the next section through the existence of a transversal homoclinic point.

13.3. Homoclinic tangle

Another important insight from dynamical system is homoclinic tangle, first proposed by Poincare to account for the complicated behavior of evolution operator. More specifically, Smale-Birkhoff theorem suggests that the existence of a transversal homoclinic point implies the existence of an invariant Cantor set, and the dynamics on which is topologically conjugate to a m -symbol full shift. This notion of m -symbol full shift was later formalized by Smale as symbolic dynamics.

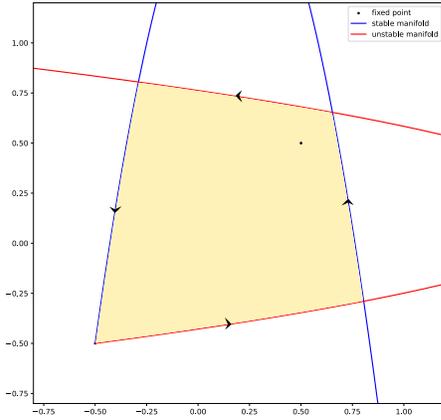
Compare to the mathematically rigorous discussion of existence of non-wandering set, this homoclinic tangle is much more intuitive, as it can be visualized through invariant manifolds, but we insisted that a detailed description of hyperbolicity and Axiom-A is necessary, as they can promote a natural way to visualize non-wandering set through intersections of a cover U of the non-wandering set. Here we propose a cover that is dynamically determined by the system, which we will call optimal cover in the following discussion.

13.4. Visualizing non-wandering set for ϕ^3 and ϕ^4

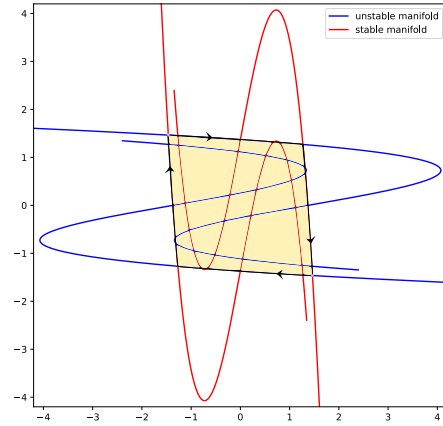
The key construction of an optimal cover of non-wandering set is to find a region that covers non-wandering set and whose boundary is invariant. This case is clearly illustrated by ϕ^3 example in Fig.2a, where the optimal cover is a region bounded by stable and unstable manifolds of fixed point origin. For ϕ^4 , it is more complicated, as stable and unstable manifold from any of the fixed points cannot bound the non-wandering set. However, considering the internal symmetry ($\phi \rightarrow -\phi$) exhibited by ϕ^4 potential, invariant manifolds are not the only invariant subset that can serve as boundary. Period-2 orbits are pairwise degenerated after quotient of internal symmetry, and a union of their corresponding invariant manifolds (which can be thought as manifolds for evolution f^2) is also an invariant subset of M under f . Thus, for ϕ^4 , optimal cover is bounded by the invariant manifolds associated with period 2 orbits, as illustrated in Fig.2b.

With the given optimal cover, approximation of non-wandering set follows 'bend and intersection' procedure of Smale's horseshoe map [[empty citation](#)], where diffeomorphism f is time evolution operator. Schematic plots Fig.3a Fig.?? show how optimal covers are bent through a "stretch and fold" process.

The conjugation of time evolution in Ω and a m -symbol full-shift is manifested by a closer look at $f(N) \cap N$ and $f^{-1}(N) \cap N$ in Fig.3. In general, time evolution of ϕ^k theory conjugates to $k-1$ symbols, as $f(N)$ is divided by N into $k-1$ simply connected regions in \mathbb{R}^2 where $k-1$ symbols can be assigned, the construction of which is reminiscent

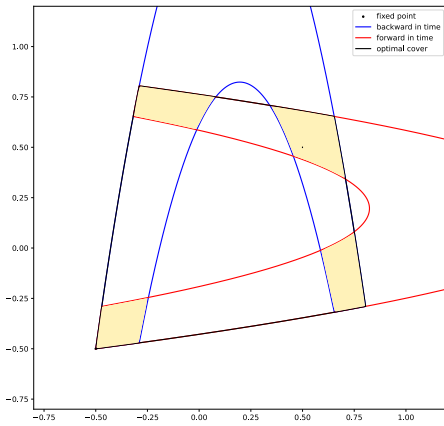


(a) Optimal cover of ϕ^3 theory with $\mu^2 = 5.5$

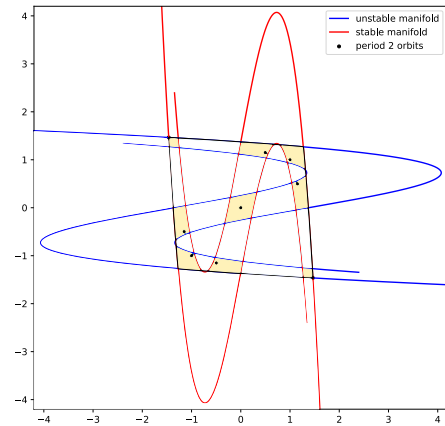


(b) Optimal cover of ϕ^4 theory with $\mu^2 = 3.5$

Figure 2: Visualization of optimal covers for ϕ^3 and ϕ^4 theory. Blue color indicates unstable manifold; red color indicates stable manifold; arrows indicates direction of expansion and contraction of invariant manifolds under time evolution f .



(a) "Stretch & fold" dynamics of ϕ^3 theory with $\mu^2 = 5.5$



(b) "Stretch & fold" dynamics of ϕ^4 theory with $\mu^2 = 3.5$

Figure 3: Schematics plots of how Ω is constructed through a dynamical process topologically equivalent to Smale's horseshoe

of Cantor set. Following the time evolution, $f^2(N) \cap N$ consists of $(k-1)^2$ simply-connected regions, with each region represented by a length-2 string with $k-1$ symbols, and $f^n(N) \cap N$ $(k-1)^n$ regions represented by length- n strings. Thus, we construct a sequence of nested sets (as finite approximations of Ω) $\{\Omega_n\}$ such that

$$\Omega_n = (f^n(N) \cap N) \cap (f^{-n}(N) \cap N), \quad (\Omega_n \subset \Omega_{n'} \forall n > n') \quad (142)$$

The structure of invariant set (which is the limit of this nested sequence) $\Omega = \lim_{n \rightarrow \infty} \bigcap \Omega_n$ is revealed by the sequence of $\{\Omega_n\}$. Write $\Omega_n = (f^n(N) \cap N) \cap (f^{-n}(N) \cap N)$, it is clear that $f^n(N) \cap N$ resembles the construction of Smale's horseshoe map, where the existence of a transversally homoclinic point guarantees that $f^n(N) \cap N$ is a disjoint union of $(k-1)^n$ simply connected regions (for ϕ^k theory, with our example taking $k = 3, 4$), each being compact. Therefore, we can label the $(k-1)^{2n}$ disjoint connected regions in Ω_n (as an intersection of $f^n(N) \cap N$ and its reversed image) by a length $2n$ string with $k-1$ symbols.

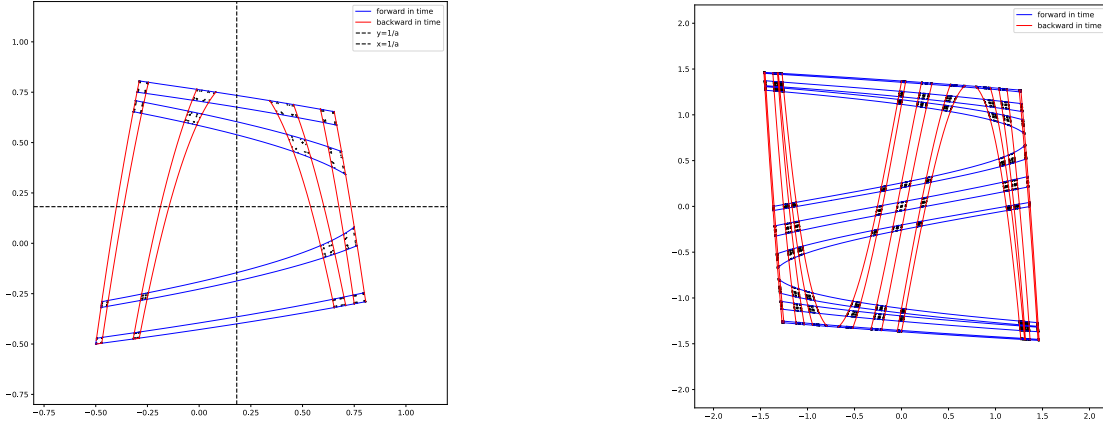
$$\Omega_n = \bigsqcup_{s \in S_n} \Omega_n^s, \quad S_n = \mathcal{A}^{2n}, \quad |\mathcal{A}| = k-1 \quad (143)$$

We arrange the symbol strings in such a way that if $s = s_{-n+1}s_{-n+2}\dots s_0s_1\dots s_n$ and $s' = s'_{-m+1}s'_{-m+2}\dots s'_0s'_1\dots s'_m$ ($n > m$) and $s_k = s'_k$ ($\forall |k| \leq m$), then $\Omega_n^s \subset \Omega_m^{s'}$ (which is possible because $\{\Omega_n\}$ is a nested sequence). Notice that we construct a Markov partition $\{\Omega_n^s\}_{s \in S_n}$ at each finite approximation Ω_n , which is the famous result prove by Bowen in 1975. With this arrangement, for each bi-infinite string $s = \dots s_{-1}s_0s_1s_2\dots \in S = \mathcal{A}^{\mathbb{Z}}$, we can construct a sequence of nested compact sets $\{\Omega_n^{s^n}\}$ where $s^n = s_{-n+1}\dots s_0s_1\dots s_n$ denote the finitely truncated substring of s of length $2n$. Let $\Omega^s = \lim_{n \rightarrow \infty} \bigcap \Omega_n^{s^n}$, by Cantor's intersection theorem Ω^s is non-empty. Since Ω is the disjoint union of Ω^s

$$\Omega = \bigsqcup_{s \in \mathcal{A}^{\mathbb{Z}}} \Omega^s \quad (144)$$

and Ω is, by its fractal nature, a totally disconnected, whose connected components are only singletons, we conclude that every orbit in Ω is uniquely represented by a bi-infinite string in S . By far, we have constructed a bijection between Ω and S , and it is clear that the time evolution (restricted on Ω) $f|_{\Omega} : \Omega \rightarrow \Omega$ is represented by a shift in S (and bijection guarantees it to be a full shift).

In this process as lies the important fact $\bar{P} = \Omega$, where P is the set of all periodic solutions and the bar means closure (mathematically speaking the smallest close set that contains P). Since the "diameter" of Ω^s decreases as the length of s increases, we can conclude that in an arbitrarily small neighborhood of $x \in \Omega \setminus P$ there is a periodic solution $c \in P$. The correspondence between \bar{P} and Ω (both as finite approximations) is shown in Fig.4 for both ϕ^3 (left panel) and ϕ^4 (right panel). This figure shows all periodic states up to period 7 and $f^2(N) \cap f^{-2}(N)$. There is a clear self-similar structure for these periodic orbits, and expected correspondence between these two sets is clear.



(a) Approximation of Ω_2 and P for ϕ^3 theory with $\mu^2 = 5.5$

(b) "Approximation of Ω_2 and P for ϕ^4 theory with $\mu^2 = 3.5$

Figure 4: Schematics plots of the correspondence between Ω and \bar{P} , where the self-similar structure of Cantor set is cleared presented

In a metric space (like \mathbb{R}^2), all the points $x \in \bar{P} \setminus P$ are said to have 'zero distance' with P , which means that for any $\delta > 0$, we can find $c \in P$ such that $d(x, c) < \delta$. We will say that c shadows x with precision δ . The existence of shadowing is the solid foundation of cycle expansion for dynamics zeta function, which will be thoroughly explored in the next section.

Through the visualization process, it is becomes clear that for a certain range of parameter (when homoclinic tangency exists), ϕ^k theory is an Axiom A flow and possess hyperbolicity on the locally maximal invariant set Ω . The dynamics on Ω is thus conjugated to a $k - 1$ symbol full shift, and this enables us to use shadowing (i.e. exploit the properties of Ω by calculation based on P) in cycle expansion of dynamical zeta function.

14. Deterministic ϕ^3 lattice field theory

To obtain a workable ϕ^3 theory we start by considering the non-Laplacian part of the action (124), with cubic Biham-Wenzel [4] lattice site potential (125)

$$V(\phi) = \frac{\mu^2}{2} \phi^2 - \frac{g}{3!} \phi^3 = -\frac{g}{3!} (\phi^3 - 3\lambda \phi^2), \quad \lambda = \mu^2/g, \quad (145)$$

parametrized by the Klein-Gordon mass $\mu > 0$ and the self-coupling constant $g \geq 0$.

Here we bring it to the anti-integrable [2, 3, 48] form, suitable for the analysis of theory's strong coupling limit.

We start by a field translation $\phi \rightarrow \phi + \epsilon$:

$$-\frac{g}{3!} ((\phi + \epsilon)^3 - 3\lambda(\phi + \epsilon)^2) = -\frac{g}{3!} (\phi^3 + 3(\epsilon - \lambda)\phi^2 + 3\epsilon(\epsilon - 2\lambda)\phi) + (\text{const}).$$

Choose the field translation $\epsilon = \lambda$, such that the ϕ^2 term vanishes,

$$-\frac{g}{3!}(\phi^3 - 3\lambda^2\phi) + (\text{const}).$$

Drop the (const) term, and rescale the field $\phi \rightarrow 2\lambda\phi$:

$$-4\lambda^2\mu^2\left(\frac{\phi^3}{3} - \frac{\phi}{4}\right).$$

As the Euler-Lagrange equations are invariant to an overall constant factor, we can ignore the overall factor of $4\lambda^2$ that appears and the ϕ^3 scalar field theory action (124) takes the form

$$S[\Phi] = \sum_z \left\{ -\frac{1}{2}\phi_z \square \phi_z - \mu^2 \left(\frac{\phi_z^3}{3} - \frac{\phi_z}{4} \right) \right\}. \quad (146)$$

The Euler–Lagrange equation (43) for the scalar lattice ϕ^3 field theory is now, in the $d = 1$ temporal lattice case

$$-\phi_{t+1} + 2\phi_t - \phi_{t-1} - \mu^2(\phi_t^2 - 1/4) = 0, \quad (147)$$

and in the d -dimensional spatiotemporal lattice case,

$$-\sum_{\|z'-z\|=1} (\phi_{z'} - \phi_z) - \mu^2(\phi_z^2 - 1/4) = 0, \quad (148)$$

parametrized by a *single* parameter, the Klein-Gordon mass μ^2 , with the ‘‘coupling constant’’ g in (124) scaled away.

Next, we compute the period-1 periodic states.

Period-1 periodic states. From the Euler–Lagrange equation (147) it follows that the period-1, constant periodic states, $\phi_t = \bar{\phi}$, for the $d = 1$ lattice are the zeros of function

$$F[\bar{\phi}] = \mu^2\left(\bar{\phi}^2 - \frac{1}{4}\right), \quad (149)$$

with two real roots $\bar{\phi}_m$

$$(\bar{\phi}_L, \bar{\phi}_R) = \left(-\frac{1}{2}, \frac{1}{2}\right). \quad (150)$$

Period-2 periodic states. To determine the four period-2 periodic states $\bar{\Phi}_m = \overline{\phi_0\phi_1}$, set $x = \phi_{2k}$, $y = \phi_{2k+1}$ in the Euler–Lagrange equation (147),

$$\mu^2(-x^2 + 1/4) + 2x - 2y = 0, \quad (151)$$

$$2\phi_1 + \mu^2(-\phi_1^2 + 1/4) - 2\phi_0 = 0, \quad (152)$$

and seek the zeros of

$$F[x, y] = \begin{pmatrix} -\mu^2(x^2 - 1/4) + 2x - 2y \\ -\mu^2(y^2 - 1/4) + 2y - 2x \end{pmatrix}. \quad (153)$$

That is best done using the Friedland and Milnor [21] ‘the center of gravity’ and Endler and Gallas [19, 20] ‘center of mass’ or ‘orbit’ polynomials, but for the period-2 periodic

states it suffices to eliminate y using $F_1 = 0 \Rightarrow 2y(x) = -\mu^2(x^2 - 1/4) + 2x$, and seek zeros of the second component,

$$F_2[x, y(x)] = -\mu^2 \left(x - \frac{1}{2}\right) \left(x + \frac{1}{2}\right) \left(\frac{\mu^4}{4}x^2 - \mu^2x + \left(2 - \frac{\mu^4}{16}\right)\right) \quad (154)$$

The first 2 roots are the $x = y$ period-1 periodic states (150) There is one period-2 periodic state $\overline{12}$

$$x, y = \pm 2\sqrt{\frac{1}{16} - 1\mu^4\mu^2 + \frac{2}{\mu^2}}, \quad (155)$$

so the prime period-2 periodic state exists for $\mu^2 > 4$. For $\mu^2 = 4$ the period-2 periodic states pairs coalesce with the positive period-1 periodic states

$$F_2[x, y(x)] = -4\left(x^2 - \frac{1}{4}\right)\left(x^2 - \frac{1}{2}\right)^2. \quad (156)$$

The first two roots are the $x = y$ period-1 periodic states (150). There is one symmetric period-2 periodic state \overline{LR}

$$x = -y = \pm\sqrt{1+??/\mu^2}, \quad (157)$$

and a pair of period-2 asymmetric periodic states $\overline{LC}, \overline{CR}$ related by reflection symmetry (time reversal).

For $\mu^2 = ??$ the period-2 asymmetric periodic states pairs coalesce with the two period-1 asymmetric periodic states

$$2x(x^2 - 3)(x^2 - 1)^3. \quad (158)$$

To get a complete horseshoe (all 2^n 2-symbol unimodal map itineraries are realized), you know what to do next (see figure 2. in [21]). Numerical work indicates [52] that for $\mu^2 > ??2.95$ the horseshoe is complete.

In the anti-integrable limit [2, 3] $\mu \rightarrow \infty$, the site field values

$$F_2[x, y(x)] \rightarrow \frac{\mu^8}{8}(x+??)^2 x^? (x-1)^? \quad (159)$$

tend to the three steady states (202).

the orbit Jacobian matrix

$$\mathcal{J}_{zz'} = -\square_{zz'} - 2\mu^2\phi_z\delta_{zz'}, \quad (160)$$

15. Deterministic ϕ^3 lattice field theory

Consider the non-Laplacian part of the action (124), with cubic Biam-Wenzel [4] lattice site potential (125)

$$V(\phi) = \frac{\mu^2}{2}\phi^2 - \frac{g}{3!}\phi^3 = -\frac{g}{3!}\left(\phi^3 - 3\lambda\phi^2\right), \quad \lambda = \mu^2/g, \quad (161)$$

parametrized by the Klein-Gordon mass $\mu > 0$ and the self-coupling constant $g \geq 0$. We will scale away one of the two parameters, in two ways. In section 15.1 we shall bring the theory to the normal, Hénon form. Here we bring it to the anti-integrable [2, 3, 48] form, suitable for the analysis of theory's strong coupling limit.

We start by a field translation $\phi \rightarrow \phi + \epsilon$:

$$-\frac{g}{3!} \left((\phi + \epsilon)^3 - 3\lambda(\phi + \epsilon)^2 \right) = -\frac{g}{3!} \left(\phi^3 + 3(\epsilon - \lambda)\phi^2 + 3\epsilon(\epsilon - 2\lambda)\phi \right) + (\text{const}).$$

Choose the field translation $\epsilon = \lambda$, such that the ϕ^2 term vanishes,

$$-\frac{g}{3!} (\phi^3 - 3\lambda^2\phi) + (\text{const}).$$

Drop the (const) term, and rescale the field $\phi \rightarrow 2\lambda\phi$:

$$-4\lambda^2\mu^2 \left(\frac{\phi^3}{3} - \frac{\phi}{4} \right).$$

The ϕ^3 scalar field theory action (124) takes form

$$S[\Phi] = \sum_z \left\{ -\frac{1}{2}\phi_z \square \phi_z - \mu^2 \left(\frac{\phi_z^3}{3} - \frac{\phi_z}{4} \right) \right\}. \quad (162)$$

The Euler–Lagrange equation (43) for the scalar lattice ϕ^3 field theory is now, in the $d = 1$ temporal lattice case

$$-\phi_{t+1} + 2\phi_t - \phi_{t-1} + \mu^2(-\phi_t^2 + 1/4) = 0, \quad (163)$$

and in the d -dimensional spatiotemporal lattice case,

$$\sum_{\|z'-z\|=1} (\phi_{z'} - \phi_z) - \mu^2 (\phi_z^2 - 1/4) = 0, \quad (164)$$

parametrized by a *single* parameter, the Klein-Gordon mass μ^2 , with the ‘‘coupling constant’’ g in (124) scaled away.

Next, we compute the period-1 and period-2 periodic states.

Period-1 periodic states. From the Euler–Lagrange equation (163) it follows that the period-1, constant periodic states, $\phi_t = \bar{\phi}$, for the $d = 1$ lattice are the zeros of function

$$F[\bar{\phi}] = \frac{4\mu^6}{g^2} \left(\bar{\phi}^2 - \frac{1}{4} \right), \quad (165)$$

with two real roots $\bar{\phi}_m$

$$(\bar{\phi}_L, \bar{\phi}_R) = \left(-\frac{1}{2}, \frac{1}{2} \right). \quad (166)$$

Period-2 periodic states. To determine the four period-2 periodic states $\bar{\Phi}_m = \overline{\phi_0\phi_1}$, set $x = \phi_{2k}$, $y = \phi_{2k+1}$ in the Euler–Lagrange equation (163), and seek the zeros of

$$F[x, y] = \begin{pmatrix} 2(x - y) - \mu^2(x^2 - 1/4) \\ 2(y - x) - \mu^2(y^2 - 1/4) \end{pmatrix}. \quad (167)$$

That is best done using the Friedland and Milnor [21] ‘the center of gravity’ and Endler and Gallas [19, 20] ‘center of mass’ or ‘orbit’ polynomials, but for the period-2 periodic states it suffices to eliminate y using $F_1 = 0 \Rightarrow y(x) = x - \frac{\mu^2}{2}(x^2 - 1/4)$, and seek zeros of the second component,

$$F_2[x, y(x)] = -\mu^2 \left(x - \frac{1}{2} \right) \left(x + \frac{1}{2} \right) \left(\frac{\mu^4}{4} x^2 - \mu^2 x + \left(2 - \frac{\mu^4}{16} \right) \right) \quad (168)$$

The first 2 roots are the $x = y$ period-1 periodic states (166). There is one period-2 periodic state $\overline{12}$

$$x, y = \frac{2 \pm 2\sqrt{\frac{\mu^4}{16} - 1}}{\mu^2}, \quad (169)$$

so the prime period-2 periodic state exists for $\mu^2 > 4$. For $\mu^2 = 4$ the period-2 periodic states pairs coalesce with the positive period-1 periodic states

$$F_2[x, y(x)] = -4\left(x^2 - \frac{1}{4}\right)\left(x^2 - \frac{1}{2}\right)^2. \quad (170)$$

In the anti-integrable limit [2, 3] $\mu \rightarrow \infty$, the site field values

$$F_2[x, y(x)] \rightarrow -\frac{\mu^6}{4}\left(x - \frac{1}{2}\right)^2\left(x + \frac{1}{2}\right)^2 \quad (171)$$

tend to the two steady states (166).

the orbit Jacobian matrix

$$\mathcal{J}_{zz'} = -\square_{zz'} - 2\mu^2\phi_z\delta_{zz'}, \quad (172)$$

15.1. Spatiotemporal lattice Hénon theory

The primary advantage of studying ϕ^3 is that it can readily be connected to the well studied temporal Hénon map **needs citations**. We can see this connection through a straightforward linear transformation. As temporal Hénon is most commonly studied in one-dimension, for the following analysis d in (164) will be set to 1. To transform between ϕ^3 and temporal Hénon we can apply the transformation $\phi_t = c\varphi_t + \varepsilon$ to (164), setting $\varepsilon = \frac{1}{\mu^2}$ yields

$$-\varphi_{t+1} - \mu^2 c \varphi_t^2 - \varphi_{t-1} = \frac{4 - \mu^4}{4\mu^2 c} = 1$$

Where the last equality is a condition enforced to maintain the form of temporal Hénon with inverted lattice values ($\varphi \rightarrow -\varphi$). Finally, we set $-\mu^2 c = a$ to recover the classical temporal Hénon parameter. Solving our two conditions and enforcing that all binary symbolic dynamics are admissible with $a = 6$, we find $c = -\frac{2}{\sqrt{3}}$ and $\mu^2 = 3\sqrt{3}$. So, the transformation which brings ϕ^3 into temporal Hénon is

$$\phi = -\frac{2}{\sqrt{3}}\varphi + \frac{1}{3\sqrt{3}} \quad (173)$$

15.2. Biham-Wenzel potential

Biham and Wenzel [4] (see **ChaosBook sect. 34.1 Fictitious time relaxation**) construct a time-asymmetric cubic action

$$S[\Phi] = \sum_{t \in \mathbb{Z}} \left(\phi_{t+1}\phi_t - b\phi_t\phi_{t-1} + \frac{a}{3}\phi_t^3 - \phi_t \right), \quad (174)$$

whose Euler–Lagrange equation is the temporal Hénon 3-term recurrence equation (??), with dissipation,

$$F_t[\Phi] = -\phi_{t+1} + b\phi_{t-1} - a\phi_t^2 + 1, \quad (175)$$

and the orbit Jacobian operator

$$\mathcal{J}_{zz'} = -r + br^{-1} - 2a\phi_t. \quad (176)$$

With the cubic potential at lattice site n we can start to look for orbits variationally. Note that the potential is time-reversal invariant for $b = 1$.

16. Deterministic ϕ^4 lattice field theory

Consider the discrete scalar one-component field, d -dimensional ϕ^4 theory [44] defined by the Euclidean action (124)

$$S[\Phi] = \sum_z \left\{ \frac{1}{2} \sum_{\mu=1}^d (\Delta_\mu \phi_z)^2 + \frac{\mu^2}{2} \phi_z^2 - \frac{g}{4!} \phi_z^4 \right\}, \quad (177)$$

with the Klein-Gordon mass $\mu \geq 0$, quartic lattice site potential (125),

$$V(\phi) = \frac{1}{2} \mu^2 \phi^2 - \frac{g}{4!} \phi^4, \quad (178)$$

the strength of the self-coupling $g \geq 0$, and we set lattice constant $a = 1$ throughout.

For a history of ϕ^4 theories in physics, see Campbell [7] *Historical overview of the ϕ^4 model* (2019). Curiously, our chaotic field theory version of the ϕ^4 theory, with the ‘inverted potential’ sign of the μ^2 nonlinear term, seems to not be even mentioned in Kevrekidis and Cuevas-Maraver [7, 29] *A Dynamical Perspective on the ϕ^4 Model: Past, Present and Future* (2019).

A popular way [35] to rewrite the quartic action (197) is to complete the square

$$V(\phi) = -\frac{g}{4!} \left(\phi_z^2 - 3! \frac{\mu^2}{g} \right)^2 + (\text{const}),$$

drop the (const) term, and rescale the field $\phi_z^2 \rightarrow 3! \frac{\mu^2}{g} \phi_z^2$:

$$S[\Phi] = 3! \frac{\mu^2}{g} \sum_z \left\{ -\frac{1}{2} \phi_z \square \phi_z - \frac{1}{4} \mu^2 (\phi_z^2 - 1)^2 \right\}. \quad (179)$$

The Euler–Lagrange equation (125) for the $d = 1$ scalar lattice ϕ^4 field theory,

$$-\phi_{t+1} + [-\mu^2 \phi_t^3 + (\mu^2 + 2) \phi_t] - \phi_{t-1} = 0, \quad (180)$$

is thus parametrized by a *single* parameter, the Klein-Gordon mass $\mu^2 = s - 2$, with the ‘coupling constant’ g in (197) scaled away. Next, we compute the period-1 and period-2 periodic states.

Period-1 periodic states. From the Euler–Lagrange equation (200) it follows that the period-1 periodic states, $\phi_t = \bar{\phi}$, for the $d = 1$ lattice are the zeros of function

$$F[\bar{\phi}] = \mu^2 (1 + \bar{\phi}) \bar{\phi} (1 - \bar{\phi}). \quad (181)$$

As long as the Klein-Gordon mass is positive, there are 3 real roots $\bar{\phi}_m$

$$(\bar{\phi}_L, \bar{\phi}_C, \bar{\phi}_R) = (-1, 0, 1). \quad (182)$$

The period-1 Bravais cell orbit Jacobian matrix \mathcal{J} is a $[1 \times 1]$ matrix

$$\mathcal{J} = s_m = \frac{dF[\phi]}{d\phi} = \mu^2 (1 - 3\bar{\phi}_m^2) = \mu^2 \text{ or } -2\mu^2, \quad (183)$$

so the "stretching" factor for the 3 steady periodic states is

$$(s_L, s_C, s_R) = (-2\mu^2, \mu^2, -2\mu^2). \quad (184)$$

Period-2 periodic states. To determine the nine period-2 periodic states $\bar{\Phi}_m = \overline{\phi_0\phi_1}$, set $x = \phi_{2k}$, $y = \phi_{2k+1}$ in the Euler–Lagrange equation (200), and seek the zeros of

$$F[x, y] = \begin{pmatrix} -(s-2)x^3 + sx - 2y \\ -(s-2)y^3 + sy - 2x \end{pmatrix}. \quad (185)$$

That is best done using the Friedland and Milnor [21] ‘the center of gravity’ and Endler and Gallas [19, 20] ‘center of mass’ or ‘orbit’ polynomials, but for the period-2 periodic states it suffices to eliminate y using $F_1 = 0 \Rightarrow 2y(x) = -x^3 + sx$, and seek zeros of the second component,

$$F_2[x, y(x)] = \frac{\mu^8}{8}(x-1)x(x+1)\left(x^2 - 1 - \frac{4}{\mu^2}\right)\left(x^4 - \left(1 + \frac{2}{\mu^2}\right)x^2 + \frac{4}{\mu^4}\right) \quad (186)$$

The first 3 roots are the $x = y$ period-1 periodic states (202). There is one symmetric period-2 periodic state \overline{LR}

$$x = -y = \pm\sqrt{1 + 4/\mu^2}, \quad (187)$$

and a pair of period-2 asymmetric periodic states $\overline{LC}, \overline{CR}$ related by reflection symmetry (time reversal).

For $\mu^2 = 2$ the period-2 asymmetric periodic states pairs coalesce with the two period-1 asymmetric periodic states

$$2x(x^2 - 3)(x^2 - 1)^3. \quad (188)$$

To get a complete horseshoe (all 3^n 3-symbol bimodal map itineraries are realized), you know what to do next (see figure 2. in [21]). Numerical work indicates [52] that for $\mu^2 > 2.95$ the horseshoe is complete.

In the anti-integrable limit [2, 3] $\mu \rightarrow \infty$, the site field values

$$F_2[x, y(x)] \rightarrow \frac{\mu^8}{8}(x+1)^3 x^3 (x-1)^3 \quad (189)$$

tend to the three steady states (202).

the orbit Jacobian matrix

$$\mathcal{J}_{zz'} = -\square_{zz'} + \mu^2(1 - 3\phi_z^2)\delta_{zz'}. \quad (190)$$

16.1. Forward in time formulation of ϕ^4

To match with Henon's formulation of ϕ^3 theory, it is inspiring to rewrite the second order difference equation of ϕ^4 theory (200) (with 1 spatiotemporal dimension) into two first order equations. The 'two-configuration representation' (reference) $\hat{\phi}_t = (\varphi_t, \phi_t)$, where $\varphi_t = \phi_{t-1}$. Then, the forward-in-time map can be written has a system of equations

$$\phi_{t+1} = -\mu^2\phi_t^3 + (\mu^2 + 2)\phi_t - \varphi_t \quad (191)$$

$$\varphi_{t+1} = \phi_t \quad (192)$$

or simply in two-configuration representation

$$\hat{\phi}_{t+1} = \begin{pmatrix} \phi_t \\ -\mu^2\phi_t^3 + (\mu^2 + 2)\phi_t - \varphi_t \end{pmatrix} \quad (193)$$

Now, assume that a periodic solution $\Phi = \overline{\phi_1\phi_2\dots\phi_n}$ is given, by notation above a sequence of vectors $(\hat{\phi}_1, \hat{\phi}_2, \dots, \hat{\phi}_n)$ (let $\phi_0 = \phi_n$) is associated with this solution. For a discrete dynamical system, the stability of a solution must come along with the solution to make anything meaningful. Locally, stability is represented by how neighborhood is distorted by time-forward map. A deviation with two-configuration representation is defined as

$$\Delta\phi_k = \begin{pmatrix} \Delta\varphi_k \\ \Delta\phi_k \end{pmatrix} = \begin{pmatrix} \Delta\phi_{k-1} \\ \Delta\phi_k \end{pmatrix} \quad (194)$$

Two deviation vectors (also true for non-periodic states) are associated with forward-in-time Jacobian matrix

$$\Delta\phi_{k+1} = \mathbb{J}_k\Delta\phi_k \quad (195)$$

which is defined as

$$\mathbb{J}_t = \begin{pmatrix} 0 & 1 \\ -1 & -\mu^2\phi_t^3 + (\mu^2 + 2)\phi_t \end{pmatrix} \quad (196)$$

For a periodic state Φ , a finite sequence of Jacobian matrices $(\mathbb{J}_1, \mathbb{J}_2, \dots, \mathbb{J}_n)$. This sequence of Jacobian matrices for periodic orbits is extremely useful in calculation of cyclic expansion, and it is closely related to the stability on lattice. Dynamics of periodic orbits are evaluated by the finite product of expanding eigenvalues of this sequence (reference). Notice that matrices \mathbb{J}_k depends on the lattice set given, so this other formulation doesn't turn a global non-linear theory into a linear one. However, it does make local calculation easier (if not making it possible), which will be discussed later.

17. Deterministic ϕ^4 lattice field theory

Consider the discrete scalar one-component field, d -dimensional ϕ^4 theory [44] defined by the Euclidean action (124)

$$S[\Phi] = \sum_z \left\{ \frac{1}{2} \sum_{\mu=1}^d (\Delta_\mu \phi_z)^2 + \frac{\mu^2}{2} \phi_z^2 - \frac{g}{4!} \phi_z^4 \right\}, \quad (197)$$

with the Klein-Gordon mass $\mu \geq 0$, quartic lattice site potential (125),

$$V(\phi) = \frac{1}{2} \mu^2 \phi^2 - \frac{g}{4!} \phi^4, \quad (198)$$

the strength of the self-coupling $g \geq 0$, and we set lattice constant $a = 1$ throughout.

A popular way [35] to rewrite the quartic action (197) is to complete the square

$$V(\phi) = -\frac{g}{4!} \left(\phi_z^2 - 3! \frac{\mu^2}{g} \right)^2 + (\text{const}),$$

drop the (const) term, and rescale the field $\phi_z^2 \rightarrow 3! \frac{\mu^2}{g} \phi_z^2$:

$$S[\Phi] = 3! \frac{\mu^2}{g} \sum_z \left\{ -\frac{1}{2} \phi_z \square \phi_z - \frac{1}{4} \mu^2 (\phi_z^2 - 1)^2 \right\}. \quad (199)$$

The Euler–Lagrange equation (125) for the $d = 1$ scalar lattice ϕ^4 field theory,

$$-\phi_{t+1} + [-\mu^2 \phi_t^3 + (\mu^2 + 2) \phi_t] - \phi_{t-1} = 0, \quad (200)$$

is thus parametrized by a *single* parameter, the Klein-Gordon mass $\mu^2 = s - 2$, with the “coupling constant” g in (197) scaled away. Next, we compute the period-1 and period-2 periodic states.

Period-1 periodic states. From the Euler–Lagrange equation (200) it follows that the period-1 periodic states, $\phi_t = \bar{\phi}$, for the $d = 1$ lattice are the zeros of function

$$F[\bar{\phi}] = \mu^2 (1 + \bar{\phi}) \bar{\phi} (1 - \bar{\phi}). \quad (201)$$

As long as the Klein-Gordon mass is positive, there are 3 real roots $\bar{\phi}_m$

$$(\bar{\phi}_L, \bar{\phi}_C, \bar{\phi}_R) = (-1, 0, 1). \quad (202)$$

The period-1 primitive cell orbit Jacobian matrix \mathcal{J} is a $[1 \times 1]$ matrix

$$\mathcal{J} = d_m = \frac{dF[\phi]}{d\phi} = \mu^2 (1 - 3\bar{\phi}_m^2) = \mu^2 \text{ or } -2\mu^2, \quad (203)$$

so the “stretching” factor for the 3 steady periodic states is

$$(d_L, d_C, d_R) = (-2\mu^2, \mu^2, -2\mu^2). \quad (204)$$

Period-2 periodic states. To determine the nine period-2 periodic states $\overline{\Phi}_m = \overline{\phi_0\phi_1}$, set $x = \phi_{2k}$, $y = \phi_{2k+1}$ in the Euler–Lagrange equation (200), and seek the zeros of

$$F[x, y] = \begin{pmatrix} -(s-2)x^3 + sx - 2y \\ -(s-2)y^3 + sy - 2x \end{pmatrix}. \quad (205)$$

That is best done using the Friedland and Milnor [21] ‘the center of gravity’ and Endler and Gallas [19, 20] ‘center of mass’ or ‘orbit’ polynomials, but for the period-2 periodic states it suffices to eliminate y using $F_1 = 0 \Rightarrow 2y(x) = -x^3 + sx$, and seek zeros of the second component,

$$F_2[x, y(x)] = \frac{\mu^8}{8}(x-1)x(x+1)\left(x^2 - 1 - \frac{4}{\mu^2}\right)\left(x^4 - \left(1 + \frac{2}{\mu^2}\right)x^2 + \frac{4}{\mu^4}\right) \quad (206)$$

The first 3 roots are the $x = y$ period-1 periodic states (202). There is one symmetric period-2 periodic state \overline{LR}

$$x = -y = \pm\sqrt{1 + 4/\mu^2}, \quad (207)$$

and a pair of period-2 asymmetric periodic states $\overline{LC}, \overline{CR}$ related by reflection symmetry (time reversal).

For $\mu^2 = 2$ the period-2 asymmetric periodic states pairs coalesce with the two period-1 asymmetric periodic states

$$2x(x^2 - 3)(x^2 - 1)^3. \quad (208)$$

To get a complete horseshoe (all 3^n 3-symbol bimodal map itineraries are realized), you know what to do next (see figure 2. in [21]). Numerical work indicates [52] that for $\mu^2 > 2.95$ the horseshoe is complete.

In the anti-integrable limit [2, 3] $\mu \rightarrow \infty$, the site field values

$$F_2[x, y(x)] \rightarrow \frac{\mu^8}{8}(x+1)^3 x^3 (x-1)^3 \quad (209)$$

tend to the three steady states (202).

18. Shadow state, temporal Hénon

Have: a partition of state space $\mathcal{M} = \mathcal{M}_A \cup \mathcal{M}_B \cup \dots \cup \mathcal{M}_Z$, with regions \mathcal{M}_m labelled by an $|\mathcal{A}|$ -letter finite alphabet $\mathcal{A} = \{m\}$. The simplest example is temporal Hénon partition into two regions, labelled ‘0’ and ‘1’,

$$m_t \in \mathcal{A} = \{0, 1\}, \quad (210)$$

plotted in figure 5 (b). Prescribe a symbol block \mathbf{M} over a finite primitive cell of a d -dimensional lattice. A 1-dimensional example:

$$\mathbf{M} = (m_0, \dots, m_{n-1}). \quad (211)$$

Want: the periodic state $\Phi_{\mathbf{M}}$ whose lattice site fields ϕ_t lie in state space domains $\phi_t \in \mathcal{M}_m$, as prescribed by the given symbol block \mathbf{M} . A 1-dimensional example:

$$\Phi_{\mathbf{M}} = (\phi_0, \dots, \phi_{n-1}), \quad \phi_t \in \mathcal{M}_m, \quad (212)$$

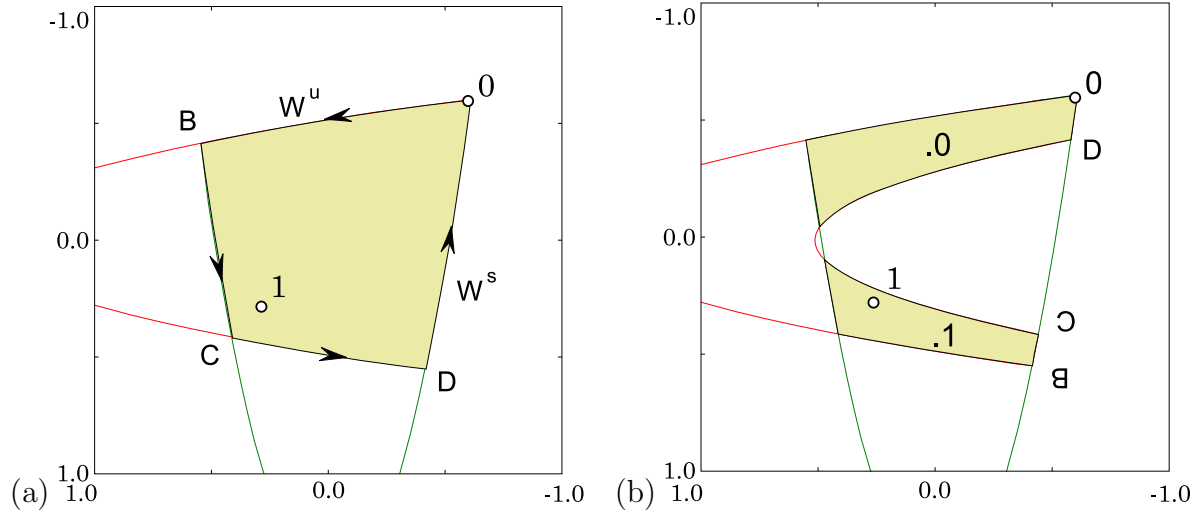


Figure 5: Temporal Hénon (A.1), (??) stable-unstable manifolds Smale horseshoe partition in the (ϕ_t, ϕ_{t+1}) plane for $a = 6$, $b = -1$: fixed point $\bar{0}$ with segments of its stable, unstable manifolds W^s , W^u , and fixed point $\bar{1}$. The most positive field value is the fixed point ϕ_0 . The other fixed point ϕ_1 has negative stability multipliers, and is thus buried inside the horseshoe. (a) Their intersection bounds the region $\mathcal{M}_0 = 0BCD$ which contains the non-wandering set Ω . (b) The intersection of the forward image $f(\mathcal{M}_0)$ with \mathcal{M}_0 consists of two (future) strips $\mathcal{M}_0, \mathcal{M}_1$, with points BCD brought closer to fixed point $\bar{0}$ by the stable manifold contraction. (The same as [ChaosBook fig. 15.5](#), with $\phi_t = -x_t$.)

By *periodic state* Φ we mean a point in the n -dimensional state space that is a solution of the defining Euler–Lagrange equation. For the temporal Hénon example, that equation is the 3-term recurrence (??),

$$-\phi_{t+1} + a\phi_t^2 - \phi_{t-1} = j_t, \quad j_t = 1, \quad (213)$$

with all $a = 6$ period-5 periodic states plotted in figure A1.

Shadow state method. Periodic states are the skeleton for dynamics in the uniformly invariant subset, thus it is necessary that we have a systematic algorithm to find periodic states numerically. One of the most powerful method among such is shadow state method, which involves constructing a shadow state based on symbolic dynamics as the initial guess and the minimize the deviation function.

Construct a *shadow state* $\bar{\Phi}_M$ and the *forcing* $j(M)_t$ such that the site-by-site deviation

$$\varphi_t = \phi_t - \bar{\phi}_t \quad (214)$$

is small. Determine the desired periodic state Φ_M as the neighboring $|\Phi_M - \bar{\Phi}_M|$ fixed point of the M -forced Euler–Lagrange equation.

Desideratum: Plot the first, $n = 6$ temporal Hénon asymmetric periodic state Φ_M and shadow state $\bar{\Phi}_M$, to illustrated the idea.

$m_{t-1}m_t m_{t+1}$	$\bar{j}(\mathbf{M})_t$
0 0 0	0
0 0 1 = 1 0 0	-A = $\bar{\phi}_1 - \bar{\phi}_0$
0 1 0	-B = $a(\bar{\phi}_1^2 - \bar{\phi}_0^2)$
1 0 1	B = $a(\bar{\phi}_0^2 - \bar{\phi}_1^2)$
1 1 0 = 0 1 1	A = $\bar{\phi}_0 - \bar{\phi}_1$
1 1 1	0

Table 1: Temporal Hénon fixed-points shadow state $\bar{\Phi}_{\mathbf{M}}$ forcing $\bar{j}(\mathbf{M})_t$ depends on the t lattice site and its two neighbors $m_{t-1}m_t m_{t+1}$. It takes values $(0, \pm A, \pm B)$. If period-2 or longer periodic states are utilized as shadows, more neighbors contribute.

First, determine the fixed points (solutions with a constant field on all lattice sites) $\phi_t = \bar{\phi}_m$. For temporal Hénon there are two, $\bar{\phi}_0$ and $\bar{\phi}_1$ (see figure 5), labeled by the alphabet (210).

Next, construct the simplest configuration from $|\mathcal{A}|$ fields $\bar{\phi}_m$, each field in the domain of state space prescribed by the symbol block \mathbf{M} . In the shadow state method, we pick a fixed point $\bar{\phi}_m$ in each domain as domain's representative $\bar{\phi}_m \in \mathcal{M}_m$. For the temporal Hénon example, the fixed-points *shadow state* is:

$$\bar{\Phi}_{\mathbf{M}} = (\bar{\phi}_0, \dots, \bar{\phi}_{n-1}), \quad \text{where } \bar{\phi}_t = \begin{cases} \bar{\phi}_0 & \text{if } m_t = 0 \\ \bar{\phi}_1 & \text{if } m_t = 1 \end{cases}. \quad (215)$$

In general, the shadow state $\bar{\Phi}_{\mathbf{M}}$ does not satisfy the Euler–Lagrange equation (213), violating it by amount $\bar{j}(\mathbf{M})_t$

$$-\bar{\phi}_{t+1} + a\bar{\phi}_t^2 - \bar{\phi}_{t-1} = 1 - \bar{j}(\mathbf{M})_t, \quad (216)$$

where the forcing $\bar{j}(\mathbf{M})_t$ depends on $\bar{\phi}_t$ and its neighbors. For the temporal Hénon example, it takes the values tabulated in table 2.

Subtract (225) from (213) to obtain the 3-term recurrence for $\varphi_t = \phi_t - \bar{\phi}_t$, the deviations (223) from the shadow state,

$$-\varphi_{t+1} + a(\phi_t^2 - \bar{\phi}_t^2) - \varphi_{t-1} = \bar{j}(\mathbf{M})_t.$$

Substituting $\phi_t^2 = (\varphi_t + \bar{\phi}_t)^2$ and $j(\mathbf{M})_t = \bar{j}(\mathbf{M})_t - a\bar{\phi}_t^2$, we obtain

M-forced Euler–Lagrange equation

for the deviation $\varphi_{\mathbf{M}}$ from the shadow lattice state configuration $\bar{\Phi}_{\mathbf{M}}$:

$$-\varphi_{t+1} + a(\varphi_t + \bar{\phi}_t)^2 - \varphi_{t-1} = j(\mathbf{M})_t. \quad (217)$$

This is to be solved by whatever code you find optimal. For example:

Vattay inverse iteration (C.1) is now

$$\varphi_t^{(m+1)} = -\bar{\phi}_t + \sigma_t \frac{1}{\sqrt{a}} \left(j(\mathbf{M})_t + \varphi_{t+1}^{(m)} + \varphi_{t-1}^{(m)} \right)^{1/2}, \quad (218)$$

and that should converge like a ton of rocks.

Perhaps watch  *Shadow state conspiracy* (35:26 min)

Overview

- (i) The \mathbf{M} -forced Euler–Lagrange equation is *exact*, the only difference from the starting Euler–Lagrange equation (213) is that lattice fields ϕ_t have been translated by constant amounts (223) in order to center it on the \mathbf{M} -th saddlepoint ‘landscape’. There is one such \mathbf{M} -forced Euler–Lagrange equation for each admissible symbol block \mathbf{M} .
- (ii) \mathbf{M} -forced 3-term recurrence (226) is *exact*. It is superior to the original recurrence as it has built-in symbolic dynamics. The deviations $\varphi_t = \phi_t - \bar{\phi}_t$ should be small, and the topological guess based on \mathbf{M} -forcing should be robust. The recurrence can be solved by any method you like.
- (iii) ϕ^4 field theory works the same, with the \mathbf{M} -forced 3-term recurrence for the deviations φ_t now built from approximate 3-field values $(\bar{\phi}_L, \bar{\phi}_C = 0, \bar{\phi}_R)$. If using Vattay (227), the Hénon sign σ_t needs to be rethought.
- (iv) Implement \mathbf{M} -forced 3-term recurrence for symmetric states boundary conditions.
- (v) Generalization to higher spatiotemporal dimensions is immediate (see, for example, the 2-dimensional Vattay iteration (C.3)).
- (vi) As one determines larger and larger primitive cell periodic states, one can use the already computed ones instead of the initial $(\bar{\phi}_0, \bar{\phi}_1)$ to get increasingly better M -forced shadowing.
- (vii) The boring forcing term $j_t = 1$ on RHS of the temporal Hénon recurrence (213) has been replaced by a non-trivial forcing $j(\mathbf{M})_t$ in (226), as hoped for.
- (viii) This is not the Biham-Wentzel method: it’s based on exact Euler–Lagrange equations, there are no artificially inverted potentials, as we are not constructing an attractor; all our solutions are and should be unstable.
- (ix) The Newton method requires evaluation of the orbit Jacobian matrix \mathcal{J} . As we have only *translated* field values $\phi_t \rightarrow \varphi_t$, \mathcal{J} is the same as for the original 3-term recurrence. For large periodic states variational methods discussed below should be far superior to simple Newton.
- (x) Have a look at Fourier transform of (226). Anything gained in Fourier space? Remember, we have not quotiented translation symmetry, we are still computing n periodic states on the spatiotemporal lattice.
- (xi) Shadowing method was first formulated by Kai Hansen [24] in *Alternative method to find orbits in chaotic systems* (1995).

19. Shadow state, ϕ^3

Have: a partition of state space $\mathcal{M} = \mathcal{M}_A \cup \mathcal{M}_B \cup \dots \cup \mathcal{M}_Z$, with regions \mathcal{M}_m labelled by an $|\mathcal{A}|$ -letter finite alphabet $\mathcal{A} = \{m\}$. The simplest example is temporal ϕ^3 theory (which can be easily mapped into temporal Hénon via [put equation here](#)) which partitions its domain into two regions, labelled ‘0’ and ‘1’,

$$m_t \in \mathcal{A} = \{0, 1\}, \quad (219)$$

plotted in figure 5 (b). We can prescribe a symbol block \mathbf{M} over a finite primitive cell of a d -dimensional lattice. A 1-dimensional example is:

$$\mathbf{M} = (m_0, \dots, m_{n-1}). \quad (220)$$

Want: the periodic state $\Phi_{\mathbf{M}}$ whose lattice site fields ϕ_t lie in state space domains $\phi_t \in \mathcal{M}_m$, as prescribed by the given symbol block \mathbf{M} . The one-dimensional temporal lattice case:

$$\Phi_{\mathbf{M}} = (\phi_0, \dots, \phi_{n-1}), \quad \phi_t \in \mathcal{M}_m, \quad (221)$$

By *periodic state* Φ we mean a point in the n -dimensional state space that is a solution of the defining Euler–Lagrange equation. For the ϕ^3 example, that equation is the 3-term recurrence (??),

$$-\phi_{t+1} + 2\phi_t - \phi_{t-1} + \mu^2 \left(-\phi_t^2 + \frac{1}{4} \right) = j_t, \quad j_t = 0, \quad (222)$$

with all $a = 6$ period-5 periodic states plotted in figure A1 ([needs to be changed to \$\phi^3\$](#)).

Shadow state method. Construct a *shadow state* $\bar{\Phi}_{\mathbf{M}}$ and the *forcing* $j(\mathbf{M})_t$ such that the site-by-site deviation

$$\varphi_t = \phi_t - \bar{\phi}_t \quad (223)$$

is small. Determine the desired periodic state $\Phi_{\mathbf{M}}$ as the neighboring $|\Phi_{\mathbf{M}} - \bar{\Phi}_{\mathbf{M}}|$ fixed point of the \mathbf{M} -forced Euler–Lagrange equation.

Desideratum: Plot the first, $n = 6$ temporal Hénon asymmetric periodic state $\Phi_{\mathbf{M}}$ and shadow state $\bar{\Phi}_{\mathbf{M}}$, to illustrate the idea.

First, determine the fixed points (solutions with a constant field on all lattice sites) $\phi_t = \bar{\phi}_m$. For temporal ϕ^3 there are two, $\bar{\phi}_0$ and $\bar{\phi}_1$ (see figure 5), labeled by the alphabet (210).

Next, construct the simplest configuration from $|\mathcal{A}|$ fields $\bar{\phi}_m$, each field in the domain of state space prescribed by the symbol block \mathbf{M} . In the shadow state method, we pick a fixed point $\bar{\phi}_m$ in each domain as domain’s representative $\bar{\phi}_m \in \mathcal{M}_m$. For the temporal ϕ^3 example, the fixed-points *shadow state* is:

$$\bar{\Phi}_{\mathbf{M}} = (\bar{\phi}_0, \dots, \bar{\phi}_{n-1}), \quad \text{where } \bar{\phi}_t = \begin{cases} \bar{\phi}_0 & \text{if } m_t = 0 \\ \bar{\phi}_1 & \text{if } m_t = 1 \end{cases}. \quad (224)$$

$m_{t-1}m_t m_{t+1}$	$\bar{j}(\mathbf{M})_t$
0 0 0	0
0 0 1 = 1 0 0	-A = $\bar{\phi}_1 - \bar{\phi}_0$
0 1 0	-B = $2(\bar{\phi}_0 - \bar{\phi}_1) + \mu^2(\bar{\phi}_1^2 - \bar{\phi}_0^2)$
1 0 1	B = $2(\bar{\phi}_1 - \bar{\phi}_0) + \mu^2(\bar{\phi}_0^2 - \bar{\phi}_1^2)$
1 1 0 = 0 1 1	A = $\bar{\phi}_0 - \bar{\phi}_1$
1 1 1	0

Table 2: Temporal ϕ^3 fixed-points shadow state $\bar{\Phi}_M$ forcing $\bar{j}(\mathbf{M})_t$ depends on the t lattice site and its two neighbors $m_{t-1}m_t m_{t+1}$. It takes values $(0, \pm A, \pm B)$. If period-2 or longer periodic states are utilized as shadows, more neighbors contribute.

In general, the shadow state $\bar{\Phi}_M$ does not satisfy the Euler–Lagrange equation (213), violating it by amount $\bar{j}(\mathbf{M})_t$

$$-\phi_{t+1} + 2\phi_t - \phi_{t-1} + \mu^2 \left(-\phi_t^2 + \frac{1}{4} \right) = -\bar{j}(\mathbf{M})_t, \quad (225)$$

where the forcing $\bar{j}(\mathbf{M})_t$ depends on $\bar{\phi}_t$ and its neighbors. For the temporal ϕ^3 example, it takes the values tabulated in table 2.

Subtract (225) from (213) to obtain the 3-term recurrence for $\varphi_t = \phi_t - \bar{\phi}_t$, the deviations (223) from the shadow state,

$$-\varphi_{t+1} + 2\varphi_t - \varphi_{t-1} + \mu^2 (-\phi_t^2 + \bar{\phi}_t^2) = \bar{j}(\mathbf{M})_t.$$

Substituting $\phi_t^2 = (\varphi_t + \bar{\phi}_t)^2$ and $j(\mathbf{M})_t = \bar{j}(\mathbf{M})_t + a\bar{\phi}_t^2$, we obtain

M-forced Euler–Lagrange equation

for the deviation φ_M from the shadow lattice state configuration $\bar{\Phi}_M$:

$$-\varphi_{t+1} + 2\varphi_t - \varphi_{t-1} - \mu^2 (\varphi_t + \bar{\phi}_t)^2 = j(\mathbf{M})_t. \quad (226)$$

This is to be solved by whatever code you find optimal. For example:

Vattay inverse iteration (C.1) is now

$$\varphi_t^{(m+1)} = -\bar{\phi}_t + \sigma_t \frac{1}{\sqrt{a}} \left(j(\mathbf{M})_t + \varphi_{t+1}^{(m)} + \varphi_{t-1}^{(m)} \right)^{1/2}, \quad (227)$$

and that should converge like a ton of rocks.

Perhaps watch  *Shadow state conspiracy* (35:26 min)

19.1. Primitive cell stability of a shadow periodic state

Comparing with the free field (91) orbit Jacobian matrix,

$$\mathcal{J}_{zz'} = -\square_{zz'} + \mu^2 \delta_{zz'},$$

the effective shadow state, site dependent Klein-Gordon masses in orbit Jacobian operators for ϕ^3 (172) are $\pm\mu^2$ (see (172), seems to conflict: check!), and for ϕ^4 (190) either μ^2 or $-2\mu^2$ (see (203)),

$$\overline{\mathcal{J}}_{zz'} = -\square_{zz'} + \overline{\mu}_z^2 \delta_{zz'}, \quad \overline{\mu}_z^2 = m_z \mu^2, \quad m_z \in \{-1, 1\}, \quad (228)$$

$$\overline{\mathcal{J}}_{zz'} = -\square_{zz'} + \overline{\mu}_z^2 \delta_{zz'}, \quad \overline{\mu}_z^2 = (1 - 3|m_z|) \mu^2, \quad m_z \in \{-1, 0, 1\}. \quad (229)$$

In the anti-integrable, strong coupling regime, one can drop the Laplacian in $\text{Det } \overline{\mathcal{J}}_p$, so the shadow Hill determinant is approximately the product of the above lattice-site dependent masses, and the shadow stability exponent is

$$\text{Det } \overline{\mathcal{J}}_p = \prod_z^{\mathbb{A}} \overline{\mu}_z^2, \quad \overline{\lambda}_p = \frac{2}{N_{\mathbb{A}}} \sum_z^{\mathbb{A}} \ln |\overline{\mu}_z|, \quad (230)$$

so for ϕ^3 and spatiotemporal cat the anti-integrable limit of shadow stability exponent is periodic state-independent, simply $\overline{\lambda}_p = \ln \mu^2$, while for ϕ^4 theory $\overline{\lambda}_p$ depends on the number of '0's in periodic state's mosaic.

20. Symbol mosaic

In the theory of dynamical systems, symbolic dynamics is a powerful tool for systematically encoding distinct temporal orbits by their symbolic itineraries. Here we briefly review the symbolic dynamics for temporal dynamical systems, then generalize this method to spatiotemporal problems, where the symbol sequences are replaced by 'mosaics', d -dimensional symbols arrays, which represent spatiotemporal periodic states globally in the spacetime [8, 9, 13, 22, 23, 36, 37].

Mosaics represents orbits by arrays of letters from a finite alphabet. Count of admissible mosaics is a convenient way to count periodic states. Consider the map of ϕ^4 field theory as an example. In section 13.2 we show that the non-wandering set of the map is bounded and the map has a three-fold horseshoe, which intersects with the optimal cover of the non-wandering set in three separated regions. The non-wandering set in the state space can be partitioned by the three strips of the horseshoe, with each region labeled by a symbol in the three-letter alphabet $\{-1, 0, 1\}$. We choose the Klein-Gordon mass μ^2 large enough such that the horseshoe of the map is complete, so every symbol sequence corresponds to one periodic orbit of the system.

Given the symbol sequences, there are many different numerical methods that can find the corresponding periodic orbits, from the simplest Newton method, to more sophisticated approaches, such as Biham and Wenzel [4] method, Hansen [24] method, Vattay [11] 'inverse iteration' method and Sterling [49] 'anti-integrable continuation' method. All of these methods require a good initial starting point, so that they converge to the periodic orbit corresponding to the given symbol sequence. A good initial point can be constructed using the symbol sequence. For the map of ϕ^4 field theory with sufficiently large μ^2 , using the pseudo-orbit consists of the fixed points corresponding to the symbols in the symbol sequence is already good enough to find the periodic orbit.

For spatiotemporal dynamical systems such as the spatiotemporal cat, spatiotemporal ϕ^3 and ϕ^4 field theory, the symbolic representation of periodic states can be given by symbol arrays, instead of symbol sequences. We refer to the symbol array as the *mosaic*. For a d -dimensional spatiotemporal system, the mosaic \mathbf{M}_c of a periodic state Φ_c is a d -dimensional symbol array:

$$\mathbf{M}_c = \{m_z\}, \quad m_z \in \mathcal{A}, \quad z \in \mathbb{Z}^d, \quad (231)$$

where \mathcal{A} is the alphabet of the symbols. Instead of treating the spatiotemporal systems as coupled maps and partitioning the high-dimensional state space, here we assign the global symbolic mosaics using the continuation from the anti-integrable limit of the systems, following the symbolic coding of Sterling *et al* [48–50] for coupled Hénon map lattice.

Consider the spatiotemporal ϕ^3 (162) and ϕ^4 (199) as examples. At the anti-integrable limit where the Klein-Gordon mass $\mu^2 \rightarrow \infty$, the ϕ^3 and ϕ^4 field theories are no longer deterministic. The temporal and spatial coupling becomes insignificant compare to the local potential, so the local field values do not depend on their neighbors, and the periodic states of the systems are arbitrary arrays of field values from a set of anti-integrable states, $\{-1/2, 1/2\}$ for ϕ^3 theory (162), and $\{-1, 0, 1\}$ for ϕ^4 theory (199). Using the set of the anti-integrable states as the symbolic alphabet \mathcal{A} , Sterling *et al* [48–50] showed that for single and coupled Hénon map, every symbol mosaic \mathbf{M}_c corresponds to an unique periodic state Φ_c which is contained in a neighborhood of \mathbf{M}_c , providing that the system is sufficiently close to the anti-integrable limit. Applying this symbolic coding to spatiotemporal ϕ^3 and ϕ^4 field theories, we have a 2-letter alphabet for ϕ^3 theory and a 3-letter alphabet for ϕ^4 theory. In this paper we choose sufficiently large Klein-Gordon mass μ^2 such that every symbol mosaic is admissible in our desired spatiotemporal domain. The mosaics are close to the corresponding periodic states, hence they are good initial starting points for numerically finding the periodic states.

21. Symmetry

All the chaotic field theories that we have examined in this and our companion papers [LC21,CL18] can be written as

$$-\square\Phi + s[\Phi] = \mathbf{M} \quad (232)$$

Where $s[\Phi]$ changes depending on what theory we are using. This can, in turn, be written as matrix multiplication

$$(-\square + \mathcal{J}[\Phi])\Phi = \mathbf{M} \quad (233)$$

Using the definition of a physical law being invariant

$$F(\Phi) = g^{-1}F(g\Phi) \quad (234)$$

By inspection, we know that $g^{-1}\square g = \square$ for all elements in C_∞ and D_∞ , next we note that in the basis where all lattice states have been rotated or reflected by some element

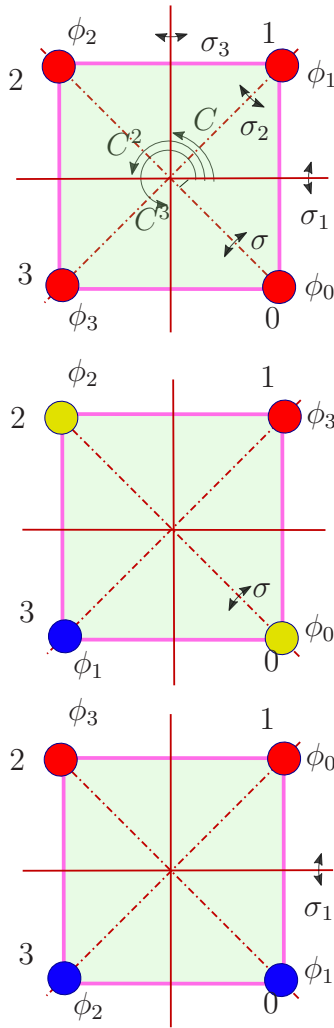


Figure 6: (Color online) Dihedral group D_4 , the group of all symmetries (236) that overlie a square onto itself, consists of 3 rotations C^k that permute the sites cyclically, and 4 rotate-reflect elements σ_k that reflect the square across reflection axes, exchanging the red and the blue sites. An even reflection (long diagonal, dashed line reflection axis), here σ , leaves a pair of opposite sites fixed (marked yellow), while an odd reflection axis (short diagonal, full line), here σ_1 , bisects the opposite edges, and flips all sites.

of D_∞ the appropriate orbit Jacobian is $\mathcal{J}[g\Phi]$ with this in mind, carrying through with (234) shows that the cat map, ϕ^3 , and ϕ^4 are all invariant under D_∞ . Realizing that our lattice equations have inherent symmetries is extremely useful. We can utilize them to speed up calculations, and make deeper theoretical observations...as long as we understand the symmetries we are working with.

21.1. Symmetries of the square lattice

The unit cell of the integer lattice (??) tiles a hypercubic lattice under action of d commuting translations (??), called ‘shifts’ for infinite lattices, ‘rotations’ for finite

periodic lattices. They form the abelian *translation group* $T = \{r_j^k \mid j = 1, 2, \dots, d, k \in \mathbb{Z}\}$, where $r_j^0 = \mathbb{1}_j$ denotes the identity, and $r_j, r_j^2, \dots, r_j^k, \dots$ denote translations by $1, 2, \dots, k, \dots$ lattice sites in the j th spatiotemporal direction. For a square lattice, the translation group consists of the product of two commuting infinite cyclic groups $T = C_{\infty,1} \otimes C_{\infty,2}$, with

$$C_{\infty,j} = \{\dots, r_j^{-2}, r_j^{-1}, \mathbb{1}, r_j^1, r_j^2, r_j^3, \dots\} \quad (235)$$

in the j th direction.

For space groups, the cosets by translation subgroup T form the *factor* (also known as *quotient*) group G/T , isomorphic to the point group g .

The Euler–Lagrange equations that define the spatiotemporal lattice field theories of section ?? are invariant under the discrete spacetime translations; the space σ_1 and time σ_3 reflections $n \rightarrow -n, t \rightarrow -t$; as well as under σ and σ_2 exchanges $n \longleftrightarrow t$ of space and time. They thus have the point-group symmetries of the square lattice: rotation C by $\pi/2$, reflections σ_1 across space-axis, σ_3 across time-axis, and σ_0, σ_2 across the two spacetime diagonals,

$$D_4 = \{e, C, C^2, C^4, \sigma_1, \sigma_3, \sigma_0, \sigma_2\}, \quad (236)$$

see figure 6. In the international crystallographic notation, this square lattice space group of symmetries is referred to as $p4mm$ [15].

Classifying periodic states by their factor group G/T is already not a simple undertaking in one temporal dimension (the subject of paper I), where it amounts to a purely group-theoretic reduction of the time reversal symmetry. While D_4 is the point group (236) of the unit square, each Bravais lattice (??) has its own factor group G/T , and -for purposes of this exposition- classifying them would lead us far from our main thrust. Here we shall construct the partition function and its reciprocal lattice representation in terms of prime periodic states, assuming only the $T = C_{\infty,1} \otimes C_{\infty,2}$ space and time translational invariance of system’s Euler–Lagrange equations. The cost of ignoring the point-group symmetries is overcounting reflection-symmetric periodic states.

21.2. Internal symmetries

In addition to section 21.1 spacetime ‘geometrical’ symmetries: invariance of the shape of a periodic state under coordinate translations, rotations, and reflections, a field theory might have *internal* symmetries, groups of transformations that leave the Euler–Lagrange equations invariant, but act only on a lattice site *field*, not on site’s location in the spacetime lattice.

For example, the ϕ^4 Euler–Lagrange equation (12) is invariant under the D_1 reflection $\phi_z \rightarrow -\phi_z$, and the spatiotemporal cat (10) is invariant under D_1 inversion of the field though the center of the $0 \leq \phi_z < 1$ unit interval:

$$\bar{\phi}_z = 1 - \phi_z \pmod{1}, \quad \text{for all } j \in \mathcal{L}, \quad (237)$$

and the corresponding inversion of lattice site symbol m_z . If $\Phi = \{\phi_z\}$ is a periodic state of the system, its inversion $\bar{\Phi} = \{\bar{\phi}_z\}$ is also a periodic state. So every periodic state of either belongs to a pair of asymmetric periodic states $\{\Phi, \bar{\Phi}\}$, or is symmetric under the inversion.

In principle, the internal symmetries should also be taken care of, but to keep the exposition simple, they are not quotiented in this paper.

21.3. What are ‘periodic states’? Orbits?

For evolution-in-time, every period- n periodic point is a fixed point of the n th iterate of the 1 time-step map. In the lattice formulation, the totality of finite-period periodic states is the *set of fixed points* of all $H_{\mathbf{a}}$ and $H_{\mathbf{a},k}$ subgroups of D_∞ .

Definition: Orbit or G -orbit of a periodic state Φ is the set of all periodic states

$$\mathcal{M}_\Phi = \{g\Phi \mid g \in G\} \tag{238}$$

into which Φ is mapped under the action of group G . We label the orbit \mathcal{M}_Φ by any periodic state Φ belonging to it.

Definition: Symmetry of a solution. We shall refer to the maximal subgroup $G_\Phi \subseteq G$ of actions which permute periodic states within the orbit \mathcal{M}_Φ , but leave the orbit invariant, as the symmetry G_Φ of the orbit \mathcal{M}_Φ ,

$$G_\Phi = \{g \in G \mid g\mathcal{M}_\Phi = \mathcal{M}_\Phi\}. \tag{239}$$

An orbit \mathcal{M}_Φ is G_Φ -symmetric (*symmetric, set-wise symmetric, self-dual*) if the action of elements of G_Φ on the set of periodic states \mathcal{M}_Φ reproduces the orbit.

Definition: Index of orbit \mathcal{M}_Φ is given by

$$m_\Phi = |G|/|G_\Phi| \tag{240}$$

(see Wikipedia [51] and Dummit and Foote [18]).

And now, a pleasant surprise, obvious upon an inspection of figures ?? and ??: what happens in the primitive cell, stays in the primitive cell. Even though the lattices \mathcal{L} , $\mathcal{L}_{\mathbf{a}}$ are infinite, and their symmetries D_∞ , $H_{\mathbf{a}}$, $H_{\mathbf{a},k}$ are *infinite* groups, the Bravais periodic states’ *orbits* are *finite*, described by the finite group permutations of the infinite lattice curled up into a primitive cell periodic n -site ring.

22. Summary

How to think about matters spatiotemporal?

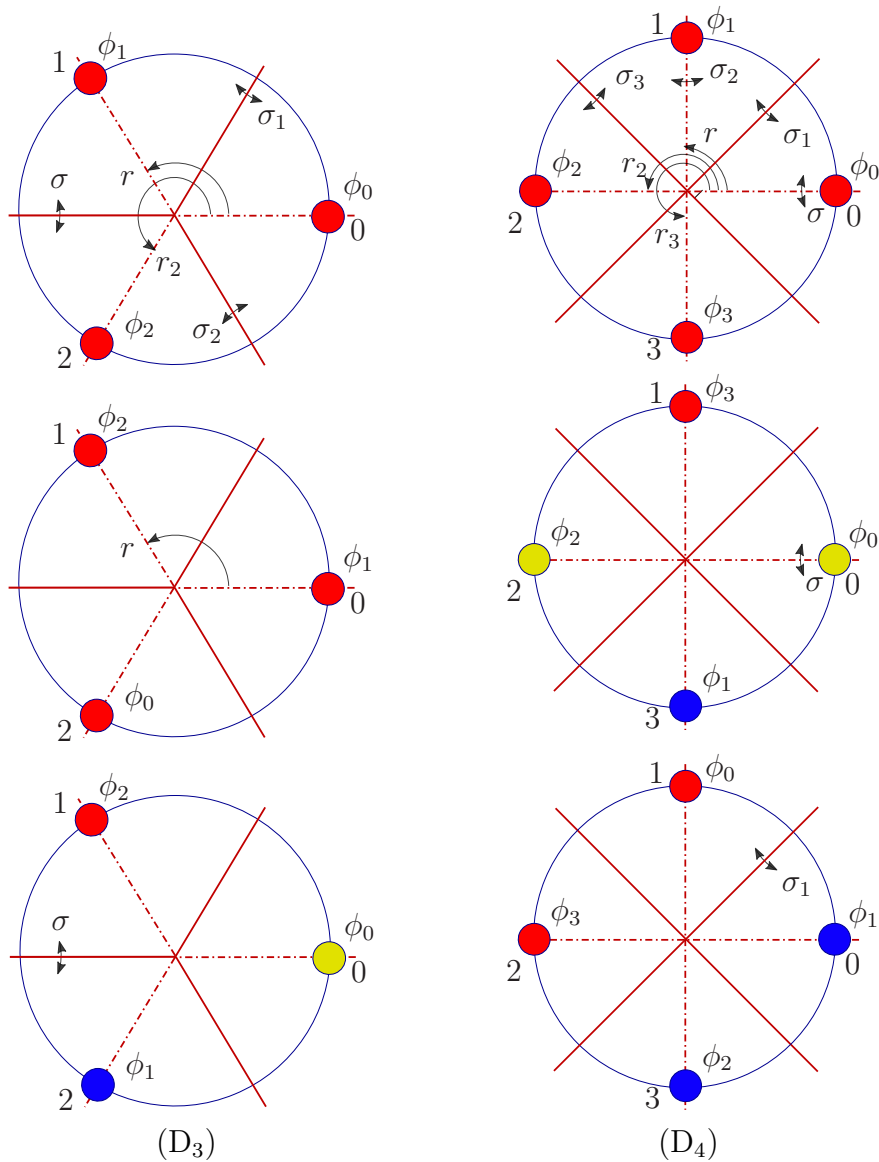


Figure 7: (Color online) Consider a period- n primitive cell tiling of a one-dimensional lattice \mathcal{L} . With \mathcal{L} curled into a ring of n lattice sites, actions of the infinite dihedral group D_∞ reduce to translational and reflection symmetries of (D_3) an equilateral triangle, $n = 3$ lattice sites; (D_4) a square, $n = 4$ lattice sites; all group operations that overlie an n -sided regular polygon onto itself. The n translations r_j permute the sites cyclically. The n dihedral group D_n translate-reflect σ_k elements (??) reflect the sites across reflection axes, exchanging red and blue sites. For even n , an even reflection (dashed line reflection axis), here σ , leaves a pair of opposite sites fixed (marked yellow), while an odd reflection axis (full line), here σ_1 , bisects the opposite edges, and flips all sites. For odd n , every reflection half-axis leaves a site fixed (dashed line), and bisects the opposite edge (full line). This periodic ring visualization makes it obvious that any symmetric periodic state is reflection invariant across two points on the lattice, see figure ??.

Acknowledgments

We are grateful to [...] . No actual cats, graduate or undergraduate were harmed during this research.

Appendix A. Spatiotemporal Hénon

The simplest nonlinear field theory with polynomial potential, the scalar ϕ^3 theory, turns out to be the spacetime generalization of the paradigmatic dynamicist's model of a two-dimensional nonlinear dynamical system, the quadratic Hénon map [26]

$$\begin{aligned} x_{t+1} &= 1 - a x_t^2 + b y_t \\ y_{t+1} &= x_t. \end{aligned} \tag{A.1}$$

For the contraction parameter value $b = -1$ this is an area-preserving, Hamiltonian map. The Hénon map is the simplest map that captures chaos that arises from the smooth stretch & fold dynamics of nonlinear return maps of flows such as Rössler [43].

The map can be interpreted as a kicked driven anaharmonic oscillator [25], with the nonlinear, cubic Biham-Wenzel [4] lattice site potential (125)

$$V(\phi) = \frac{1}{2} \mu^2 \phi^2 - \frac{1}{3!} g \phi^3, \tag{A.2}$$

so we refer to this field theory as ϕ^3 theory. A parameter can be rescaled away by translations and rescalings of the field ϕ , and the Euler–Lagrange equation of the system can be brought to various equivalent forms, such as the Hénon form (A.3), or the anti-integrable form (A.4),

Written as a 2nd-order inhomogeneous difference equation [17], (A.1) takes the nearest-neighbor Laplacian form, the Euler–Lagrange equation (43),

$$-\square\varphi_z + a\varphi_z^2 - 2d\varphi_z + 1 = 0. \tag{A.3}$$

To bring this to a form more convenient for our purposes, complete the square,

$$-\square\varphi_z - a \left[\left(\varphi_z + \frac{d}{a} \right)^2 - \frac{d^2 + a}{a^2} \right] = 0,$$

and rescale the field as $\varphi = -A\phi$,

$$-\square\phi_z - aA \left[\left(\phi_z + \frac{d}{aA} \right)^2 - \frac{d^2 + a}{(aA)^2} \right] = 0.$$

To cast this into the anti-integrable form pick a convenient set of roots, for example the symmetric pair $(1/2, -1/2)$, separated by 1. Then $(aA)^2 = 4(a + d^2)$. Calling that parameter the ‘Klein-Gordon mass squared’ μ^2 , the Euler–Lagrange equation takes the anti-integrable form, with the potential dominating for large μ^2 ,

$$-\square\phi_z + \mu^2 (1/4 - \phi_z^2) = 0. \tag{A.4}$$

To compare our results with the extensive, single temporal dimension, we note that the Hénon stretching parameter a in (A.3) and the Klein-Gordon mass μ^2 in (A.4) are related by

$$\mu^2 = 2\sqrt{a+1}. \tag{A.5}$$

For a sufficiently large ‘stretching parameter’ a , or ‘mass parameter’ μ^2 , the periodic states of this ϕ^3 theory are in one-to-one correspondence to the unimodal Hénon map Smale horseshoe repeller, cleanly split into the ‘left’, positive stretching and ‘right’, negative stretching lattice site field values. A plot of such horseshoe, given in, for example, [ChaosBook Example 15.4](#), is helpful in understanding that state space of deterministic solutions of strongly nonlinear field theories has fractal support. Devaney, Nitecki, Sterling and Meiss [14, 48, 50] have shown that the Hamiltonian Hénon map has a complete Smale horseshoe for stretching parameter a or Klein-Gordon mass μ^2 values (A.5) above

$$a > 5.699310786700\dots \tag{A.6}$$

$$\mu^2 > 5.17660536904\dots \tag{A.7}$$

In numerical [11] and analytic [20] calculations ChaosBook fixes the stretching parameter value to $a = 6$, $\mu^2 = 5.29150262213$, in order to guarantee that all 2^n periodic points $\phi = f^n(\phi)$ of the Hénon map (A.1) exist.

The symbolic dynamics is binary.

Appendix B. Inverse iteration method

(Gábor Vattay, Sidney V. Williams and P. Cvitanović)

The ‘inverse iteration method’ for determining the periodic orbits of 2-dimensional repeller was introduced by G. Vattay as a [ChaosBook.org Inverse iteration method for a Hénon repeller](#). The idea of the method is to

- (1) Guess a lattice configuration $\phi_t^{(0)}$ that qualitatively looks like the desired periodic state. For that, you need a qualitative, symbolic dynamics description of system’s admissible periodic states. You can get started by a peak at [ChaosBook Table 18.1](#).
- (2) Compare the ‘stretched’ field $\phi_t^{(0)}$ to its neighbors, using system’s defining equation. For example, ϕ^3 (or temporal Hénon) Euler–Lagrange equation (163) is

$$-\phi_{t+1} - \left(\mu^2 \phi_t^2 - 2\phi_t + \frac{\mu^2}{4} \right) - \phi_{t-1} = 0.$$

Perhaps watch  [What’s ”The Law”?](#) (4 min).

- (3) Use the amount by which ϕ_t ‘sticks out’ in violation of the defining equations to obtain a better value $\phi_t^{(1)}$, for every lattice site t . Vattay does that by inverting the equation, determining $\phi_t^{(1)}$ from its neighbors

$$\phi_t^{(m+1)} = \sigma_t \frac{1}{\sqrt{a}} \left(1 + \phi_{t+1}^{(m)} + \phi_{t-1}^{(m)} \right)^{1/2} \tag{B.1}$$

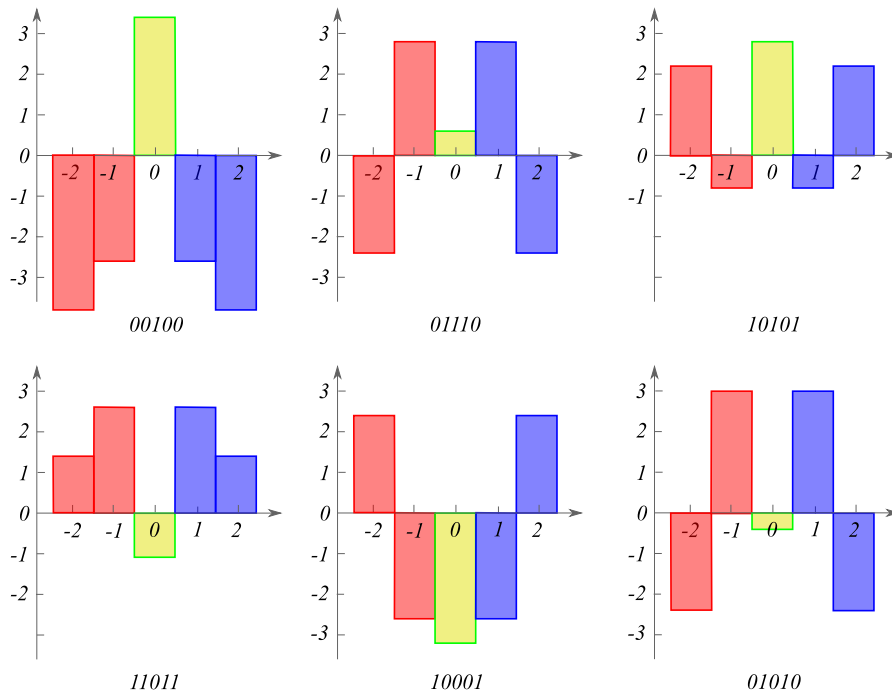


Figure A1: Temporal Hénon (??), $a = 6$: All period $n = 5$ prime periodic states $\phi_{-2}\phi_{-1}\phi_0\phi_1\phi_2$ of table ?? . They are all reflection symmetric, with the fixed lattice field ϕ_0 colored gold. The most striking feature is how far the $a = 6$ temporal Hénon is from the $0 \leftrightarrow 1$ symmetry: stretching close to $\bar{0}$ fixed point periodic state is much stronger than close to the almost marginal $\bar{1}$ fixed point periodic state. For a stretching parameter value a slight lower than the critical value $a_h = 5.69931\dots$, the lattice sites ϕ_0 for $\overline{01110}$ and $\overline{01010}$ coalesce and vanish through an inverse bifurcation. As $a \rightarrow \infty$ we expect this symmetry to be restored.

where σ_t is the sign of the target site field $\sigma_t = \phi_t/|\phi_t|$, prescribed in advance by specifying the desired Hénon symbol block

$$\sigma_t = 1 - 2m_t, \quad m_t \in \{0, 1\}. \tag{B.2}$$

Perhaps watch [Inverse iteration method](#) (14:28 min).

- (4) Wash and repeat, $\phi_t^{(m)} \rightarrow \phi_t^{(m+1)}$. Sidney starts the iteration by setting the initial guess lattice site fields to

$$\phi_t^{(0)} = \sigma_t/\sqrt{a},$$

and then loops (C.1) through all lattice site fields to obtain $\phi_t^{(1)}$. When $|\phi_t^{(m+1)} - \phi_t^{(1)}|$ for all periodic states is smaller than a desired tolerance, the loop terminates, and the periodic state is found. An example of the resulting periodic states is given in figure A1.

The meat of the method is contained in these two loops:

```
for i in range(0,len(symbols)):
    cycle[i]=signs[i]*np.sqrt(abs(1-np.roll(cycle,1)[i]-np.roll(cycle,-1)[i])/a)
```

```
for i in range(0,len(symbols)):
```

```
    deviation[i]=np.roll(cycle,-1)[i]-(1-a*(cycle[i])**2-np.roll(cycle,1)[i])
```

The method applies to strongly coupled ϕ^3 field theory in any spatiotemporal dimension. For example, in 2 spacetime dimensions, the m th inverse iterate (C.1) compares the ‘stretched’ field $\phi_{nt}^{(0)}$ to its 4 neighbors,

$$\phi_{nt}^{(m+1)} = \sigma_{nt} \frac{1}{\sqrt{2a}} \left(2 + \phi_{n,t+1}^{(m)} + \phi_{n,t-1}^{(m)} + \phi_{n+1,t}^{(m)} + \phi_{n-1,t}^{(m)} \right)^{1/2}. \quad (\text{B.3})$$

It is applied to each of the LT lattice site fields $\{\phi_{nt}^{(m)}\}$ of a doubly periodic primitive cell $[L \times T]_S$. Here σ_{nt} is the sign of the target site field $\sigma_{nt} = \phi_{nt}/|\phi_{nt}|$, prescribed in advance by specifying the desired Hénon symbol block \mathbf{M} ,

$$\sigma_{nt} = 1 - 2m_{nt}, \quad m_{nt} \in \{0, 1\}. \quad (\text{B.4})$$

For the *temporal Hénon* 3-term recurrence (??), the system’s state space Smale horseshoe is again generated by iterates of the region plotted in figure 5. So, positive field ϕ_{nt} value has $m_{nt} = 0$, negative field ϕ_{nt} value has $m_{nt} = 1$.

Appendix C. Inverse iteration method

(Gábor Vattay, Sidney V. Williams and P. Cvitanović)

The ‘inverse iteration method’ for determining the periodic orbits of 2-dimensional repeller was introduced by G. Vattay as a ChaosBook.org *Inverse iteration method for a Hénon repeller*. The idea of the method is to

- (1) Guess a lattice configuration $\phi_t^{(0)}$ that qualitatively looks like the desired periodic state. For that, you need a qualitative, symbolic dynamics description of system’s admissible periodic states. You can get started by a peak at [ChaosBook Table 18.1](#).
- (2) Compare the ‘stretched’ field $\phi_t^{(0)}$ to its neighbors, using system’s defining equation. For example, ϕ^3 (or temporal Hénon) Euler–Lagrange equation (163) is

$$-\phi_{t+1} - \left(\mu^2 \phi_t^2 - 2\phi_t + \frac{\mu^2}{4} \right) - \phi_{t-1} = 0.$$

Perhaps watch  *What’s ”The Law”?* (4 min).

- (3) Use the amount by which ϕ_t ‘sticks out’ in violation of the defining equations to obtain a better value $\phi_t^{(1)}$, for every lattice site t . Vattay does that by inverting the equation, determining $\phi_t^{(1)}$ from its neighbors

$$\phi_t^{(m+1)} = \sigma_t \frac{1}{\sqrt{a}} \left(1 + \phi_{t+1}^{(m)} + \phi_{t-1}^{(m)} \right)^{1/2} \quad (\text{C.1})$$

where σ_t is the sign of the target site field $\sigma_t = \phi_t/|\phi_t|$, prescribed in advance by specifying the desired Hénon symbol block

$$\sigma_t = 1 - 2m_t, \quad m_t \in \{0, 1\}. \quad (\text{C.2})$$

Perhaps watch  *Inverse iteration method* (14:28 min).

- (4) Wash and repeat, $\phi_t^{(m)} \rightarrow \phi_t^{(m+1)}$. Sidney starts the iteration by setting the initial guess lattice site fields to

$$\phi_t^{(0)} = \sigma_t / \sqrt{a},$$

and then loops (C.1) through all lattice site fields to obtain $\phi_t^{(1)}$. When $|\phi_t^{(m+1)} - \phi_t^{(1)}|$ for all periodic states is smaller than a desired tolerance, the loop terminates, and the periodic state is found. An example of the resulting periodic states is given in figure A1.

The meat of the method is contained in these two loops:

```
for i in range(0,len(symbols)):
    cycle[i]=signs[i]*np.sqrt(abs(1-np.roll(cycle,1)[i]-np.roll(cycle,-1)[i])/a)
for i in range(0,len(symbols)):
    deviation[i]=np.roll(cycle,-1)[i]-(1-a*(cycle[i])**2-np.roll(cycle,1)[i])
```

The method applies to strongly coupled ϕ^3 field theory in any spatiotemporal dimension. For example, in 2 spacetime dimensions, the m th inverse iterate (C.1) compares the ‘stretched’ field $\phi_{nt}^{(0)}$ to its 4 neighbors,

$$\phi_{nt}^{(m+1)} = \sigma_{nt} \frac{1}{\sqrt{2a}} \left(2 + \phi_{n,t+1}^{(m)} + \phi_{n,t-1}^{(m)} + \phi_{n+1,t}^{(m)} + \phi_{n-1,t}^{(m)} \right)^{1/2}. \quad (\text{C.3})$$

It is applied to each of the LT lattice site fields $\{\phi_{nt}^{(m)}\}$ of a doubly periodic primitive cell $[L \times T]_S$. Here σ_{nt} is the sign of the target site field $\sigma_{nt} = \phi_{nt}/|\phi_{nt}|$, prescribed in advance by specifying the desired Hénon symbol block M ,

$$\sigma_{nt} = 1 - 2 m_{nt}, \quad m_{nt} \in \{0, 1\}. \quad (\text{C.4})$$

For the *temporal Hénon* 3-term recurrence (??), the system’s state space Smale horseshoe is again generated by iterates of the region plotted in figure 5. So, positive field ϕ_{nt} value has $m_{nt} = 0$, negative field ϕ_{nt} value has $m_{nt} = 1$.

References

- [1] S. Anastassiou, A. Bountis, and A. Bäcker, “Homoclinic points of 2D and 4D maps via the parametrization method”, *Nonlinearity* **30**, 3799–3820 (2017).
- [2] S. Aubry, “Anti-integrability in dynamical and variational problems”, *Physica D* **86**, 284–296 (1995).
- [3] S. Aubry and G. Abramovici, “Chaotic trajectories in the standard map. The concept of anti-integrability”, *Physica D* **43**, 199–219 (1990).
- [4] O. Biham and W. Wenzel, “Characterization of unstable periodic orbits in chaotic attractors and repellers”, *Phys. Rev. Lett.* **63**, 819 (1989).
- [5] T. Bountis and R. H. G. Helleman, “On the stability of periodic orbits of two-dimensional mappings”, *J. Math. Phys.* **22**, 1867–1877 (1981).
- [6] R. Bowen, “Markov partitions for Axiom A diffeomorphisms”, *Amer. J. Math.* **92**, 725–747 (1970).

- [7] D. K. Campbell, Historical overview of the ϕ^4 model, in *A Dynamical Perspective on the ϕ^4 Model* (Springer, 2019) Chap. 1, pp. 1–22.
- [8] S.-N. Chow, J. Mallet-Paret, and W. Shen, “Traveling waves in lattice dynamical systems”, *J. Diff. Equ.* **149**, 248–291 (1998).
- [9] S.-N. Chow, J. Mallet-Paret, and E. S. Van Vleck, “Pattern formation and spatial chaos in spatially discrete evolution equations”, *Random Comput. Dynam.* **4**, 109–178 (1996).
- [10] H. Cohen, *A Course in Computational Algebraic Number Theory* (Springer, Berlin, 1993).
- [11] P. Cvitanović, R. Artuso, R. Mainieri, G. Tanner, and G. Vattay, *Chaos: Classical and Quantum* (Niels Bohr Inst., Copenhagen, 2024).
- [12] P. Cvitanović, R. Artuso, L. Rondoni, and E. A. Spiegel, “Transporting densities”, in *Chaos: Classical and Quantum*, edited by P. Cvitanović, R. Artuso, R. Mainieri, G. Tanner, and G. Vattay (Niels Bohr Inst., Copenhagen, 2023).
- [13] P. Cvitanović and H. Liang, *A chaotic lattice field theory in two dimensions*, In preparation, 2024.
- [14] R. L. Devaney and Z. Nitecki, “Shift automorphisms in the Hénon mapping”, *Commun. Math. Phys.* **67**, 137–146 (1979).
- [15] M. S. Dresselhaus, G. Dresselhaus, and A. Jorio, *Group Theory: Application to the Physics of Condensed Matter* (Springer, New York, 2007).
- [16] D. Dudgeon and R. M. Mersereau, *Multidimensional Digital Signal Processing* (Prentice-Hall, Englewood Cliffs, NJ, 1984).
- [17] H. R. Dullin and J. D. Meiss, “Generalized Hénon maps: the cubic diffeomorphisms of the plane”, *Physica D* **143**, 262–289 (2000).
- [18] D. S. Dummit and R. M. Foote, *Abstract Algebra* (Wiley, 2003).
- [19] A. Endler and J. A. C. Gallas, “Conjugacy classes and chiral doublets in the Hénon Hamiltonian repeller”, *Phys. Lett. A* **356**, 1–7 (2006).
- [20] A. Endler and J. A. C. Gallas, “Reductions and simplifications of orbital sums in a Hamiltonian repeller”, *Phys. Lett. A* **352**, 124–128 (2006).
- [21] S. Friedland and J. Milnor, “Dynamical properties of plane polynomial automorphisms”, *Ergodic Theory Dynam. Systems* **9**, 67–99 (1989).
- [22] B. Gutkin, L. Han, R. Jafari, A. K. Saremi, and P. Cvitanović, “Linear encoding of the spatiotemporal cat map”, *Nonlinearity* **34**, 2800–2836 (2021).
- [23] B. Gutkin and V. Osipov, “Classical foundations of many-particle quantum chaos”, *Nonlinearity* **29**, 325–356 (2016).
- [24] K. T. Hansen, “Alternative method to find orbits in chaotic systems”, *Phys. Rev. E* **52**, 2388–2391 (1995).
- [25] J. F. Heagy, “A physical interpretation of the Hénon map”, *Physica D* **57**, 436–446 (1992).

- [26] M. Hénon, “A two-dimensional mapping with a strange attractor”, *Commun. Math. Phys.* **50**, 94–102 (1976).
- [27] N. S. Izmailian, K. B. Oganesyan, and C.-K. Hu, “Exact finite-size corrections for the square-lattice Ising model with Brascamp-Kunz boundary conditions”, *Phys. Rev. E* **65**, 056132 (2002).
- [28] G. Kane, *Modern Elementary Particle Physics* (Addison-Wesley, Redwood City, 1987).
- [29] P. G. Kevrekidis and J. Cuevas-Maraver, eds., *A Dynamical Perspective on the ϕ^4 Model: Past, Present and Future* (Springer, Berlin, 2019).
- [30] O. Knill and F. Tangerman, “Self-similarity and growth in Birkhoff sums for the golden rotation”, *Nonlinearity* **24**, 3115–3127 (2011).
- [31] S. Lang, *Linear Algebra* (Addison-Wesley, Reading, MA, 1987).
- [32] H. Liang and P. Cvitanović, “A chaotic lattice field theory in one dimension”, *J. Phys. A* **55**, 304002 (2022).
- [33] T. M. Liaw, M. C. Huang, Y. L. Chou, S. C. Lin, and F. Y. Li, “Partition functions and finite-size scalings of Ising model on helical tori”, *Phys. Rev. E* **73**, 041118 (2006).
- [34] D. A. Lind, “A zeta function for Z^d -actions”, in *Ergodic Theory of Z^d Actions*, edited by M. Pollicott and K. Schmidt (Cambridge Univ. Press, 1996), pp. 433–450.
- [35] M. Lüscher and P. Weisz, “Scaling laws and triviality bounds in the lattice ϕ^4 theory (I). One-component model in the symmetric phase”, *Nucl. Phys. B* **290**, 25–60 (1987).
- [36] J. Mallet-Paret and S.-N. Chow, “Pattern formation and spatial chaos in lattice dynamical systems. I”, *IEEE Trans. Circuits Systems I Fund. Theory Appl.* **42**, 746–751 (1995).
- [37] J. Mallet-Paret and S.-N. Chow, “Pattern formation and spatial chaos in lattice dynamical systems. II”, *IEEE Trans. Circuits Systems I Fund. Theory Appl.* **42**, 752–756 (1995).
- [38] I. Montvay and G. Münster, *Quantum Fields on a Lattice* (Cambridge Univ. Press, Cambridge, 1994).
- [39] G. Münster, “Lattice quantum field theory”, *Scholarpedia* **5**, 8613 (2010).
- [40] G. Münster and M. Walzl, *Lattice gauge theory - A short primer*, 2000.
- [41] Y. Okabe, K. Kaneda, M. Kikuchi, and C.-K. Hu, “Universal finite-size scaling functions for critical systems with tilted boundary conditions”, *Phys. Rev. E* **59**, 1585–1588 (1999).
- [42] P. Ramond, *Field Theory* (Routledge, 1981).
- [43] O. E. Rössler, “An equation for continuous chaos”, *Phys. Lett. A* **57**, 397–398 (1976).

- [44] H. J. Rothe, *Lattice Gauge Theories - An Introduction* (World Scientific, Singapore, 2005).
- [45] D. Ruelle, *Thermodynamic Formalism: The Mathematical Structure of Equilibrium Statistical Mechanics*, 2nd ed. (Cambridge Univ. Press, Cambridge, 2004).
- [46] C. L. Siegel and K. Chandrasekharan, *Lectures on the Geometry of Numbers* (Springer Berlin Heidelberg, Berlin, Heidelberg, 1989).
- [47] B. Simon, “Almost periodic Schrödinger operators: A review”, *Adv. Appl. Math.* **3**, 463–490 (1982).
- [48] D. Sterling and J. D. Meiss, “Computing periodic orbits using the anti-integrable limit”, *Phys. Lett. A* **241**, 46–52 (1998).
- [49] D. G. Sterling, *Anti-integrable Continuation and the Destruction of Chaos*, PhD thesis (Univ. Colorado, Boulder, CO, 1999).
- [50] D. G. Sterling, H. R. Dullin, and J. D. Meiss, “Homoclinic bifurcations for the Hénon map”, *Physica D* **134**, 153–184 (1999).
- [51] Wikipedia contributors, *Index of a subgroup — Wikipedia, The Free Encyclopedia*, 2022.
- [52] S. V. Williams, X. Wang, H. Liang, and P. Cvitanović, *Nonlinear chaotic lattice field theory*, In preparation, 2024.
- [53] U. Wolff, “Triviality of four dimensional ϕ^4 theory on the lattice”, *Scholarpedia* **9**, 7367 (2014).